The two C-terminal tyrosines stabilize occluded Na/K pump conformations containing Na or K ions

Natascia Vedovato and David C. Gadsby

Laboratory of Cardiac/Membrane Physiology, The Rockefeller University, New York, NY 10065

Interactions of the three transported Na ions with the Na/K pump remain incompletely understood. Na/K pump crystal structures show that the extended C terminus of the Na,K–adenosine triphosphatase (ATPase) α subunit directly contacts transmembrane helices. Deletion of the last five residues (KETYY in almost all Na/K pumps) markedly lowered the apparent affinity for Na activation of pump phosphorylation from ATP, a reflection of cytoplasmic Na affinity for forming the occluded E1P(Na3) conformation. ATPase assays further suggested that C-terminal truncations also interfere with low affinity Na interactions, which are attributable to extracellular effects. Because extracellular Na ions traverse part of the membrane's electric field to reach their binding sites in the Na/K pump, their movements generate currents that can be monitored with high resolution. We report here electrical measurements to examine how Na/K pump interactions with extracellular Na ions are influenced by C-terminal truncations. We deleted the last two (YY) or five (KESYY) residues in *Xenopus laevis* α1 Na/K pumps made ouabain resistant by either of two kinds of point mutations and measured their currents as 10-mM ouabain–sensitive currents in *Xenopus* oocytes after silencing endogenous *Xenopus* Na/K pumps with 1 µM ouabain. We found the low affinity inhibitory influence of extracellular Na on outward Na/K pump current at negative voltages to be impaired in all of the C-terminally truncated pumps. Correspondingly, voltage jump–induced transient charge movements that reflect pump interactions with extracellular Na ions were strongly shifted to more negative potentials; this signals a several-fold reduction of the apparent affinity for extracellular Na in the truncated pumps. Parallel lowering of Na affinity on both sides of the membrane argues that the C-terminal contacts provide important stabilization of the occluded E1P(Na3) conformation, regardless of the route of Na ion entry into the binding pocket. Gating measurements of palytoxin-opened Na/K pump channels additionally imply that the C-terminal contacts also help stabilize pump conformations with occluded K ions.

INTRODUCTION

Recent x-ray crystal structures of native Na/K pumps with enclosed K (or Rb) ions (Morth et al., 2007; Shinoda et al., 2009), together with those of the related sarcoplasmic and endoplasmic reticulum Ca (SERCA) pumps in several key conformations of the catalytic and ion transport cycle (Toyoshima et al., 2000, 2004, 2007; Toyoshima and Nomura, 2002; Olesen et al., 2004, 2007; Sørensen et al., 2004; Toyoshima and Mizutani, 2004) as well as Na/K pump homology models based on them Ogawa and Toyoshima, 2002; Rakowski and Sagar, 2003; Takeuchi et al., 2008), have deepened our understanding of the molecular mechanisms by which both pumps generate the steep cation gradients across cellular membranes that are crucial to animal cell life. The structures and models have also placed interpretations of the plethora of biochemical and physiological data obtained over the preceding decades (for reviews see Glynn, 1993; Apell and Karlish, 2001; Kaplan, 2002) on a sound structural footing. However, the structural correlates of Na/K pump events associated with its transport of three Na ions have not yet been clarified. A reasonable assumption supported by results of mutagenesis (Jorgensen and Pedersen, 2001) is that two of the Na ions bind within the transmembrane (TM) domain between helix TM5 and the unwound portions of helices TM4 and TM6, like the two K ions found in the Na/K pump crystal structures (Morth et al., 2007; Shinoda et al., 2009). Where the third Na ion binds is less clear, although atomic models (Ogawa and Toyoshima, 2002; Rakowski and Sagar, 2003) and mutagenesis (Imagawa et al., 2005; Li et al., 2005) have directed attention to a site between helices TM6, TM8, and TM9, adjacent to the first two sites.

A striking feature revealed by the Na/K pump structures (Morth et al., 2007; Shinoda et al., 2009) is that the C terminus of the α subunit is extended by some eight residues compared with that of the SERCA pump and that this extension mediates contacts that link the cytoplasmic end of TM10 to TM5, TM7, and the TM8–TM9 cytoplasmic linker (Fig. 1 A). Moreover, its truncation

Correspondence to David C. Gadsby: gadsby@rockefeller.edu

Abbreviations used in this paper: SERCA, sarcoplasmic and endoplasmic reticulum Ca; TM, transmembrane; TMA, tetramethylammonium; WT, wild type.

The Rockefeller University Press $30.00
J. Gen. Physiol. Vol. 136 No. 1 63–82
www.jgp.org/cgi/doi/10.1085/jgp.201010407

by deletion of the last five highly conserved residues, KETYY, caused a marked lowering of the apparent affinity for Na to activate Na/K pump phosphorylation by ATP to form the occluded E1P(Na3) state, reflecting impaired interaction with Na ions entering their binding sites from the cytoplasmic side (Morth et al., 2007). This raised the question of whether interactions of the Na/K pump with Na ions entering from the extracellular side were also influenced by the presence or absence of the C terminus.

Na/K pump interactions with extracellular Na (Nao) are of two kinds, as cartooned in the simplified Post-Albers (Post et al., 1965; Albers, 1967) scheme of the transport cycle of the Na/K pump modeled as an ion pathway controlled by two gates, one on each side of the ion-binding sites (Fig. 1 B). In the absence of extracellular K (Ko) ions but in the presence of external and internal Na and ATP, the ATP is hydrolyzed at a low rate (Post et al., 1972), which is first enhanced as the concentration of extracellular Na, [Nao], is raised but is then inhibited at very high [Nao] (Garrahan and Glynn, 1967; Taniguchi and Post, 1975). The interpretation is that two Nao ions, in the first of the two kinds of interactions, can act as surrogate Ko to support a low rate of pump dephosphorylation, thus driving a slow Na-ATPase cycle (not depicted). But, at sufficiently high [Nao], in the second kind of interaction, binding of a third Nao ion favors occupancy of the occluded E1P(Na3) state, further impeding completion of the ATP hydrolysis cycle. Comparable inhibition of ATPase by Nao acting with low apparent affinity occurs in the presence of Ko (Garrahan and Glynn, 1967). This low affinity inhibition of Na/K pumping by Nao is steeply voltage dependent, becoming stronger at more negative membrane potentials (Nakao and Gadsby, 1989; Sagar and Rakowski, 1994).

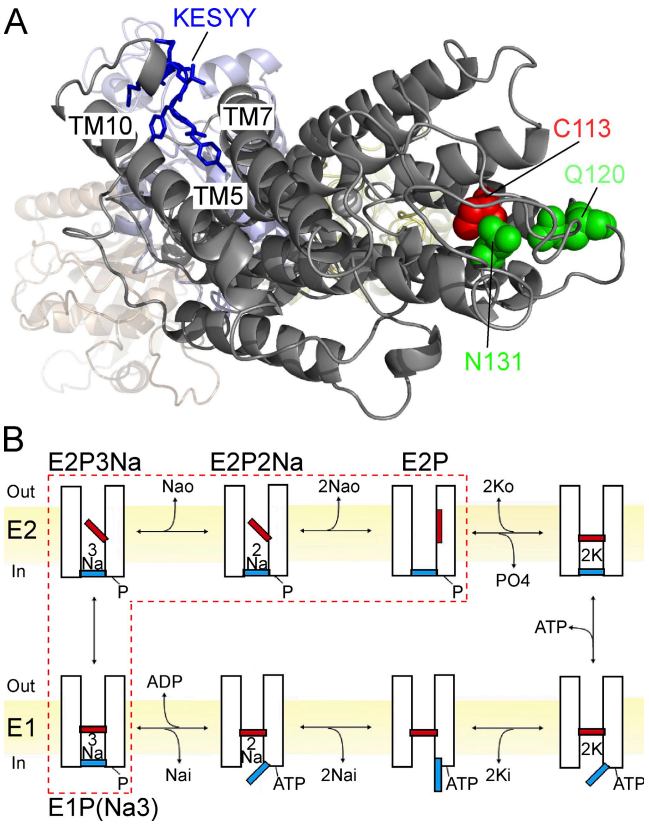

Figure 1. Structure of the Na/K pump α subunit and representation of its transport cycle. (A) Angled extracellular view of Na,K-ATPase α-subunit structure (Morth et al., 2007) indicating locations (*Xenopus* numbering) of mutations introduced here in *Xenopus* Na,K-ATPase α1 subunits to confer ouabain resistance, C113Y (red) or Q120R/N131D (green), and C-terminal truncation, ΔYY or ΔKESYY (blue). (B) Cartoon of an alternating-gate representation (Artigas and Gadsby, 2003) of the Post-Albers transport cycle of the Na/K pump, indicating E1 states with the extracellular-side gate (red) closed and cytoplasmic access to ion-binding sites and E2 states with the cytoplasmic-side gate (blue) closed and extracellular access to ion-binding sites. The dashed box encloses the phosphorylated pump conformations linked in a voltage-dependent equilibrium in the presence of saturating Nai and ATP and of Nao but in the absence of Ko.

Low affinity voltage-dependent Nao binding not only inhibits forward Na/K cycling (clockwise in Fig. 1 B) at negative voltages, but it also activates reverse Na/K pumping (anticlockwise in Fig. 1 B; De Weer et al., 2001) and electroneutral Na/Na exchange (back and forth transit between the four leftmost states in Fig. 1 B; Gadsby et al., 1993) at negative potentials. In all of these cases, analysis of the kinetic equivalence between increments in [Nao] and negative voltage shifts indicates that either maneuver facilitates Nao ion binding deep inside the pump, ∼70% of the electrical distance from the extracellular surface (Gadsby et al., 1993; Rakowski, 1993; Heyse et al., 1994; Hilgemann, 1994; Sagar and Rakowski, 1994; Wuddel and Apell, 1995). The same low affinity dependence on [Nao] and membrane potential is observed for the largest, and slowest, component of pump-mediated transient charge movement elicited by voltage jumps in the absence of Ko but in the presence of external and internal Na and of ATP (Nakao and Gadsby, 1986; Hilgemann, 1994; Wuddel and Apell, 1995; Friedrich and Nagel, 1997; Holmgren et al., 2000); the transient charge movements track the time course of redistribution of states that comprise the voltage-dependent equilibrium outlined by the dashed box in Fig. 1 B, the slow component relaxing with rates appropriate for the Nao occlusion/deocclusion step, E2P3Na ↔ E1P(Na3) (Forbush, 1984; Steinberg and Karlish, 1989). Two smaller components of the Na charge movements relax with faster time courses, and the fastest is only weakly voltage dependent (Hilgemann, 1994; Wuddel and Apell, 1995; Holmgren et al., 2000), reminiscent of the weakly voltage-sensitive binding of Ko (Rakowski et al., 1991; Stürmer et al., 1991; Berlin and Peluffo, 1997). The loss of those faster components (and concomitant growth of the slow component), after keeping the membrane potential at a negative level for longer times, signaled

the existence of reciprocal relationships between the magnitudes of the three components, which led to the conclusion that the three components reflect sequential binding/release of the three Nao ions (Holmgren et al., 2000). Together, these findings argue that the strongly voltage-dependent low affinity Nao binding is to the third site and that this rate limits the slow occlusion step.

These characteristics of Na/K pump currents make them well suited to address whether C-terminal truncation alters pump interactions with Nao and, if so, at which sites. Biochemical measurements did indeed show that C-terminal mutations interfere with the ability of high [Na] to inhibit Na-ATPase activity, which is suggestive of impaired Nao binding (Toustrup-Jensen et al., 2009). That C-terminal mutations lower the apparent affinity of Nao binding was similarly concluded from recent electrophysiological investigations (Yaragatupalli et al., 2009; Meier et al., 2010). However, those studies disagreed as to whether the impairment is in Nao binding at the two sites believed to be shared with K ions (Yaragatupalli et al., 2009) or at the special third Na site (Meier et al., 2010). In both studies, an additional current, seemingly Nao dependent, was observed to flow inwards and apparently energetically downhill through the Na/K pumps with C-terminal truncations (Yaragatupalli et al., 2009; Meier et al., 2010); the growth of this unexpected inward current at increasingly negative potentials possibly contributed to the discrepant conclusions. In this study, we present our contemporaneous analysis of the consequences of deleting the last two (YY) or five (KESYY; Fig. 1 A, blue sticks) α-subunit residues in *Xenopus laevis* Na/K pumps made ouabain resistant by two different kinds of point mutations. These allowed us to measure steady-state and transient pump currents as 10-mM ouabain–sensitive currents in *Xenopus* oocytes while endogenous *Xenopus* Na/K pumps were silenced with 1 µM ouabain. From examination of the voltage dependence of Nao influence on steady outward pump current and on transient Na charge movements, we found that the strongly, but not the weakly, voltage-dependent interactions with Nao were impaired by both C-terminal truncations. The magnitudes of these effects, together with those on interactions with cytoplasmic-side Na (Morth et al., 2007; Toustrup-Jensen et al., 2009; Yaragatupalli et al., 2009), indicate that the C-terminal tyrosines provide contacts that stabilize the occluded E1P(Na3) conformation by ∼2 kT, regardless of the side of the membrane from which Na ions enter the third binding site. Furthermore, examination of Ko-induced closure of palytoxin-bound Na/K pump channels suggests that the influence of those C-terminal contacts is not restricted to occluded Na states but that they also play a part in closure of the external gate by extracellular K ions.

MATERIALS AND METHODS

Mutagenesis and expression

Ouabain resistance–conferring point mutations Q120R/N131D (denoted RD; Price and Lingrel, 1988) or C113Y (Canessa et al., 1992) were introduced (Fig. 1 A) into the *Xenopus* Na,K-ATPase α1 subunit using QuikChange (Agilent Technologies). Deletion of the last two (YY) or five (KESYY) most C-terminal residues was performed by PCR of cDNA encoding the RD or C113Y *Xenopus* α1 Na, K-ATPase. After in vitro transcription of cDNA in *pSD5* vector, 15 ng cRNA of *Xenopus* wild-type (WT) or mutant Na,K-ATPase α1 subunit was coinjected with 5 ng *Xenopus* β3 subunit into defolliculated *Xenopus* oocytes, which were then incubated at 18°C for 2–4 d.

Solutions

The three principal external solutions contained 125 mM NaOH, tetramethylammonium (TMA)-OH, or KOH, 120 mM sulfamic acid, 10 mM HEPES, 5 mM $BaCl_2$, 1 mM $MgCl_2$, 0.5 mM $CaCl_2$, pH 7.6, plus 1 µM ouabain (10 µM for patch recordings) to avoid signals from endogenous Na/K pumps (ouabain was omitted from solutions used to record from WT Na/K pumps). Pipette (internal) solution for patch recordings contained 125 mM NaOH, 120 mM sulfamic acid, 10 mM HEPES, 1 mM $MgCl_2$, and 1 mM EGTA, pH 7.4. The osmolality of these internal and external solutions was 250–260 mosmol/Kg. K- and Ca-free solution for raising intracellular Na concentration ([Nai]) contained 95 mM NaOH, 90 mM sulfamic acid, 5 mM HEPES, 10 mM TEACl, and 0.1 mM EGTA, pH 7.6; osmolality was ∼210 mosmol/Kg. To activate Na/K exchange, up to 15 mM K-sulfamate was added (from a 1-M stock solution) to the Na- or TMA-containing external solutions. To inhibit all Na/K pump–mediated currents, 10 mM ouabain was directly dissolved into the appropriate external solution. Palytoxin (from *Palythoa tuberculosa*; Wako Pure Chemical Industries Ltd) was dissolved in aqueous 0.001% wt/vol BSA solution, and the 100-µM stock solution was stored at −20°C. Just before use, it was diluted to a final concentration of 100 nM in external Na solution supplemented with 0.001% BSA and 1 mM Na-borate.

Electrophysiology

Oocytes expressing WT or mutant Na/K pumps were examined at 22–24°C using two-microelectrode voltage clamp or excised outside-out patch recording. Whole oocyte currents were acquired with an oocyte voltage clamp amplifier (OC-725A; Warner Instruments) filtered at 1 kHz and sampled at 5 kHz with an18-bit ITC-18 A/D-D/A board controlled by Patch Master 2.20 software (Instrutech; HEKA). Before each two-microelectrode experiment, [Nai] was elevated by exposing oocytes to K-free, Ca-free, Nai-loading solution for ≥2 h at 18°C. Na/K exchange current was activated maximally by exposure to 15 mM Ko or incrementally by stepwise increase of [Ko]. Maximal Na/K pump current was estimated as current abolished by 10 mM ouabain at 15 mM [Ko], and apparent affinity for Ko interaction with the pump was determined as $K_{0.5}$(Ko) from fits to the Hill equation of Ko-sensitive current versus [Ko] in the presence or absence of 125 mM Nao at each test voltage (currents were averaged over the final 10 ms of 100-ms pulses from the −50-mV holding potential to voltages between −140 and 40 mV in 10-mV increments).

Transient Na charge movements were investigated as ouabain-sensitive pre–steady-state currents in 125 mM Nao elicited by 100-ms steps from the −50-mV holding potential to test voltages between −180 and 60 mV in 20-mV increments. Relaxation rates of transient currents were obtained from single exponential fits beginning 1–3 ms after the start of the step to each test voltage. The quantity of ouabain-sensitive pre–steady-state charge moved was determined as the time integral of the entire transient current for both "on" and "off" voltage jumps (after subtraction of any steady currents), and its voltage distribution was fitted to a Boltzmann relation.

Patch data were recorded with an amplifier (Axopatch 200B; MDS Analytical Technologies), filtered at 500 Hz, and sampled at 5 kHz with a Digidata 1200 A/D-D/A driven by pClamp7 software (MDS Analytical Technologies). Palytoxin was applied to outside-out patches held at −50 mV in symmetric 125-mM Na solutions until inward Na/K pump channel current reached a steady state, and palytoxin was then washed out. The inward current increase was fitted to a single exponential to obtain τ_{act}. Nao was then replaced by Ko (for 5–15 min) to determine the time course of Ko-induced closure of palytoxin-activated pump channels.

Data were analyzed with IgorPro 6 (WaveMetrics), ClampFit (in pClamp 9; MDS Analytical Technologies), and Origin 7.0 (Origin Laboratory). Results are reported as mean ± SEM of *n* measurements.

Online supplemental material

Fig. S1 confirms that 15 mM Ko does not influence steady-state I-V relationships in the presence of ouabain, regardless of the presence of Nao, in oocytes expressing WT, RD, or C113Y Na/K pumps. It also shows that 10 mM ouabain completely abolishes the inward current seen at negative potentials in RD or C113Y pumps in Nao- and Ko-free solution. The ouabain sensitivity of that nonstoichiometric inward current in Ko-free solutions is shown in Fig. S2 for all RD and C113Y pumps, without or with C-terminal truncations, both in the absence and presence of Nao. Fig. S3 shows the time constants of opening of palytoxin-bound pump channels for all pump types tested in this study as well as the fractions of those pump channels that shut rapidly on replacing Nao with Ko.

RESULTS

Comparison of two distinct ouabain-resistant mutants with WT Na/K pumps

As most animal cells contain highly ouabain-sensitive native Na/K pumps, mutant pumps are conveniently studied by making them relatively resistant to ouabain and then examining them in the presence of sufficient ouabain to abolish endogenous pump signals (e.g., Vilsen, 1992). Rat α1 Na,K-ATPase is naturally ouabain resistant, partly because of Gln-to-Arg and Asn-to-Asp (Fig. 1 A, green) substitutions at the external boundaries of TM1 and TM2, respectively (Price and Lingrel, 1988). A further screen for ouabain resistance identified another mutation in TM1, a Cys-to-Tyr (Fig. 1 A, red) substitution (Canessa et al., 1992). Although these substitutions all lie near the ouabain-binding site (Ogawa et al., 2009), the detailed mechanisms of their influence on ouabain binding and effects on Na/K pump function are not well understood. Before studying the additional consequences of C-terminal truncation, therefore, currents generated by mutant *Xenopus* α1β3 Na/K pumps bearing either of these two kinds of ouabain resistance–conferring mutations, Q120R/N131D (denoted RD; homologous to those used in recent studies of C-terminal mutations; Toustrup-Jensen et al., 2009; Yaragatupalli et al., 2009; Meier et al., 2010) or C113Y, were compared with those of WT *Xenopus* α1β3 Na/K pumps. In a single experiment (Fig. 2 A), currents were recorded in the same oocyte with elevated internal [Na] before and after addition of 15 mM of external K to strongly activate Na/K exchange, both in the presence and absence of external Na and with repeated strategic additions of 10 mM ouabain to inhibit all Na/K pumps. The third exposure to 15 mM [Ko] caused the same outward current shift as the first (Fig. 2 A), confirming both that sufficient time had been allowed for full recovery from the preceding application of ouabain and that [Nai] remained supersaturating throughout the experiment. Under each condition, voltage pulses (Fig. 2 A, vertical lines) were applied to sample currents (Fig. 2, B, D, and F) at membrane potentials every 20 mV over the range of −180 to 60 mV. Steady currents measured near the ends of the pulses in each condition are plotted against voltage for WT (Fig. 2 G), RD (Fig. 2 C), and C113Y (Fig. 2 E) Na/K pumps. For all three pump types, membrane current was small at all voltages when oocytes were in K-free, 125-mM [Nao] solution (Fig. 2, C, E, and G, closed squares), became more outward at all voltages upon pump activation with 15 mM [Ko] (Fig. 2, C, E, and G, closed circles), and returned to the initial control level when pumps were inhibited by addition of ouabain to the 15-mM [Ko] solution (Fig. 2, C, E, and G, closed triangles).

Because under these conditions, i.e., at 125 mM [Nao], the current activated by saturating [Ko] matched the current abolished by a maximally inhibiting [ouabain], either could provide a reliable measure of stationary outward current generated by forward Na,K-ATPase cycling for WT, RD, and C113Y pumps. The shapes of their ouabain-sensitive Na/K pump current–voltage relationships in 15 mM [Ko] and 125 mM [Nao] were similar (Fig. 3, A–D, closed symbols): they all demonstrated the diminution of current with increasingly negative potentials that is attributed to voltage-dependent inhibition of the forward Na/K exchange cycle by Nao ions being driven into binding sites deep within the membrane's electric field (Nakao and Gadsby, 1989; Rakowski et al., 1989; Sagar and Rakowski, 1994).

In the absence of Nao (Na replaced by TMA), however, maximal Ko-activated current closely matched ouabain-inhibited current only in WT pumps and not in the ouabain-resistant pumps (Fig. 2, C, E, and G, open symbols). In both RD and C113Y pumps, Ko-activated current and ouabain-inhibited current were the same only at membrane potentials more positive than −50 mV (Fig. 2, C and E, open symbols). The discrepancy between Ko-activated and ouabain-inhibited current in RD and C113Y pumps at membrane potentials more negative than −50 mV was a result of the occurrence of a large inward current at negative potentials in those pumps when Nao and Ko were both omitted (Fig. 2, C and E, open squares) that was abolished by ouabain (Fig. S1). A comparable inwardly rectifying current, inhibited by ouabain, has previously been observed in WT pumps exposed to Na- and K-free solutions at acidic pH and has been ascribed to proton flow through the pump (Efthymiadis

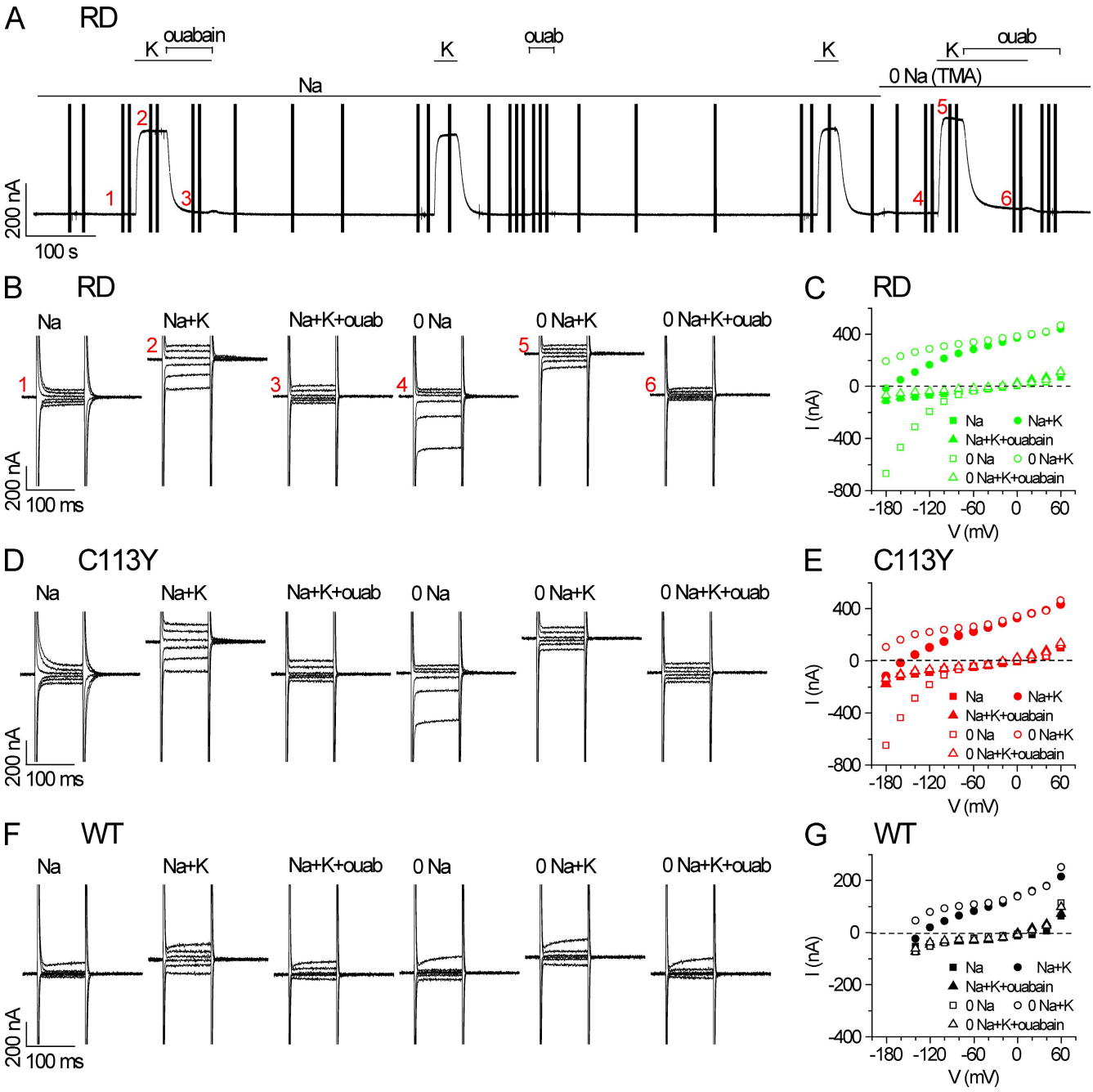

Figure 2. Determination of steady-state Na/K pump current of WT and ouabain-resistant RD and C113Y mutant pumps in the presence and absence of external Na (replaced by TMA). (A) Representative record of current changes at the −50-mV holding potential in a Na-loaded oocyte expressing RD Na/K pumps caused by addition of 15 mM Ko and/or 10 mM ouabain in the presence and then in the absence of Nao as indicated; the vertical lines mark application of 100-ms voltage steps to −180 to 60 mV in 20-mV increments. (B) Selected superimposed current traces from the experiment in A obtained at the times identified on the recording by the red numbers. Analogous traces are superimposed for C113Y (D) and WT (F) pumps. The corresponding steady-state (mean of last 10 ms of each step) current–voltage (I-V) relationships for each Na/K pump type, obtained from the records in B, D, and F, are shown in C, E, and G.

et al., 1993; Wang and Horisberger, 1995; Vasilyev et al., 2004). The fact that the ouabain-sensitive current–voltage relationships of RD and C113Y pumps at saturating 15-mM [Ko] in 0 mM [Nao] (Fig. 3, A, B, and D, open symbols) had similar shapes to that for WT pumps (Fig. 3, C and D, open symbols), which show no sign of the inward current (Fig. 2 G), suggests that the large inward current seen at negative potentials in RD and C113Y pumps in Nao- and Ko-free solution is abolished not only by ouabain (Fig. S1 and Fig. S2) but also by saturating [Ko] (Fig. 2, C and E, open circles). This suggestion will be confirmed below (see section Sensitivity to Ko of currents…) by determinations of Ko sensitivity, but for now we can conclude that the mean maximally Ko-activated

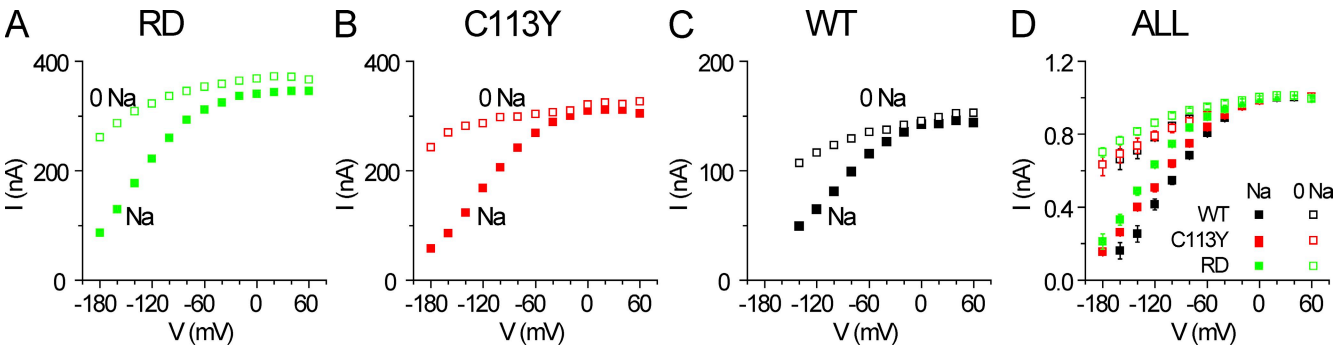

Figure 3. Voltage-dependent inhibition of steady-state outward Na/K pump current by Nao. Inhibition in RD (A), C113Y (B), and WT (C) pumps. Ouabain-sensitive currents in 15 mM Ko, without (open symbols) or with (closed symbols) external Na, were obtained by appropriate subtraction of data shown in Fig. 2 (B–G). (D) To facilitate comparison among the different pumps, each ouabain-sensitive I-V relationship was normalized to its mean amplitude between 0 and 60 mV, and the normalized I-Vs for each pump type, with or without Nao, were then averaged.

Na/K pump current–voltage relationships in Fig. 3 D are free of contamination from the inward current, even at the most negative membrane potentials. Together, they show that stoichiometrically coupled outward Na/K exchange current generated by RD or C113Y pumps, like that of WT pumps, is relatively weakly inhibited by negative voltages in the absence of Nao but strongly inhibited in 125 mM [Nao]. The RD and C113Y Na/K pumps are therefore suitable surrogates for WT pumps in which to study the influence of deleting the last five (ΔKESYY) or last two (ΔYY) C-terminal residues.

Effects of ΔYY and ΔKESYY truncations on currents in Ko-free solutions

In Nao- and Ko-free solutions, C113Y pumps with ΔKESYY or ΔYY mutations showed a large inward current at the most negative membrane potentials similar to that observed in C113Y pumps (Fig. 2 E), but, in these C-terminal mutants, an inward current of comparable magnitude was also recorded in 125-mM [Nao] solution (Fig. 4). Similarly, large inward currents in the same K-free, 125-mM [Nao] solution were also recorded in RD pumps with ΔKESYY or ΔYY mutations, but, in contrast to our observations with truncated C113Y pumps, in both RD pumps with C-terminal truncations the current was diminished approximately threefold when Nao was absent (Fig. 4; Yaragatupalli et al., 2009; Meier et al., 2010). Importantly, all inward currents at large negative potentials were abolished by ouabain; in C113Y pumps with or without the C-terminal deletions, half-maximal abolition took <50 µM ouabain, and in the corresponding RD pumps, half-maximal abolition needed ≤400 µM ouabain (Fig. S2). Moreover, for each pump type, the estimated ouabain sensitivity of outward stoichiometric Na/K exchange current was similar to that of the inward current, confirming that 10 mM ouabain was sufficient to abolish both kinds of Na/K pump–mediated current.

Sensitivity to Ko of currents in Na/K pumps without and with ΔYY and ΔKESYY truncations

To obtain information about interactions with extracellular ions, the Ko sensitivity of currents generated by each mutant Na/K pump was determined with or without Nao by stepwise increases of [Ko] up to 15 mM followed by pump inhibition with 10 mM ouabain (e.g., C113Y at 0 mM [Nao] in Fig. 5 A). Sample current–voltage relationships in Ko-free solution and at each incremental [Ko] are depicted for C113Y in Na-free solutions (Fig. 5 B) and for C113Y-ΔKESYY in 125-mM [Nao]

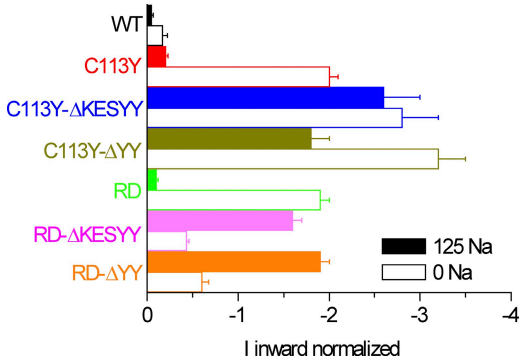

Figure 4. Comparison of the magnitude of ouabain-sensitive inward current in each pump type at −180 mV (−160 mV for WT) in the absence or presence of 125 mM Nao after normalization by the ouabain-sensitive pump current activated by 15 mM [Ko] at the −50-mV holding potential in the same oocyte and [Nao] to allow for differences in expression. Open bars, absence of 125 mM Nao; closed bars, presence of 125 mM Nao. Mean values are −0.04 ± 0.02, n = 4, in 125 mM Nao and −0.17 ± 0.05, n = 4, in 0 mM Nao for WT Na/K pumps (black); −0.20 ± 0.03, n = 8, in 125 mM Nao and −2.0 ± 0.1, n = 8, in 0 mM Nao for C113Y (red); −2.6 ± 0.4, n = 5, in 125 mM Nao and −2.8 ± 0.4, n = 5, in 0 mM Nao for C113Y-ΔKESYY (blue); −1.8 ± 0.2, n = 6, in 125 mM Nao and −3.2 ± 0.6, n = 6, in 0 mM Nao for C113Y-ΔYY (olive); −0.10 ± 0.02, n = 7, in 125 mM Nao and −1.9 ± 0.1, n = 7, in 0 mM Nao for RD (green); −1.6 ± 0.1, n = 8, in 125 mM Nao and −0.43 ± 0.03, n = 8, in 0 mM Nao for RD-ΔKESYY (magenta); and −1.9 ± 0.1, n = 7, in 125 mM Nao and −0.60 ± 0.08, n = 7, in 0 mM Nao for RD-ΔYY (orange). Error bars represent SEM.

solutions (Fig. 5 E). As already noted (Fig. 4), both of these examples show the large inward current at strong negative potentials in 0 mM [Ko]. As with WT (Fig. S1 F), RD (Fig. S1 B), and C113Y (Fig. S1 D) Na/K pumps, current–voltage relationships recorded in the presence of ouabain in oocytes expressing C-terminally truncated RD or C113Y pumps were insensitive to Ko, whether in the presence or absence of Nao. This means that only currents generated by Na/K pumps were modulated by Ko. The outward current shift upon raising [Ko] in the absence of ouabain (Fig. 5, B, C, E, and F) therefore reflects, at the most negative voltages, primarily diminution of the inward current but, at positive potentials, almost exclusively reflects activation of outward Na/K exchange current. Because 10 mM ouabain abolishes both components (Fig. 5, B and E, closed triangles), the ouabain-sensitive current–voltage relationships (Fig. 5, D and G) give their sum at each [Ko], and neither component can be resolved. On the other hand, Hill fits to the extracellular K-modulated currents at each voltage revealed that in Nao-free solutions (Fig. 5 C), the $K_{0.5}$(Ko) increased gradually from extreme negative potentials to the most positive potentials for all pump types (Fig. 5, H–J, open circles). This shallow voltage dependence of $K_{0.5}$(Ko) is attributable to Ko ions binding a small distance into the membrane's electric field (Rakowski et al., 1991; Stürmer et al., 1991; Jaisser et al., 1994; Sagar and Rakowski, 1994; Berlin and Peluffo, 1997). The $K_{0.5}$(Ko)–voltage curves are all smooth, and the weak voltage dependence of $K_{0.5}$(Ko) is broadly similar in all the pumps studied here in Nao-free solutions, including the WT Na/K pumps, which lack any inward current. This implies that the Ko sensitivity of loss of inward current is the same as that of activation of outward Na/K exchange current, which would explain the lack of discernible transition along the $K_{0.5}$(Ko)–voltage curves between the region dominated by inward current and that dominated by outward current. Therefore, we further conclude that both effects are the result of Ko binding at the same sites in the Na/K pump.

Competition between Ko and Nao in Na/K pumps without and with ΔYY or ΔKESYY truncations

The invariably larger $K_{0.5}$(Ko) values in 125 mM [Nao] than in 0 mM [Nao] (Fig. 5, F and H–J) reflect competition between Nao and Ko for binding to E2P conformations of the Na/K pumps (Fig. 1 B, top). The near parallel increases in $K_{0.5}$(Ko) with and without Nao at positive potentials can be accounted for by progressively impaired K binding within the electric field as membrane potential is made more positive, with or without competition from comparably weakly voltage-dependent (and thus similarly waning) binding of Nao (compare with Li et al., 2006). But the variably steep increase in $K_{0.5}$(Ko) at negative potentials in 125 mM [Nao] reflects inhibition caused by more strongly voltage-dependent binding of Nao at a site (or sites) deeper in the electric field (Nakao and Gadsby, 1989; Rakowski et al., 1989). As WT, RD, and C113Y pumps all lack substantial inward current in 125-mM [Nao] solutions, the overall somewhat smaller $K_{0.5}$(Ko) of RD pumps under those conditions (Fig. 5 H, closed green circles) suggests that the latter might bind Ko more tightly than WT or C113Y pumps. Nevertheless, the steep increase in $K_{0.5}$(Ko) at large negative potentials of RD pumps in 125 mM [Nao] (Fig. 5 H, closed green circles) demonstrates that they retain the strongly voltage-dependent inhibitory Nao binding of WT pumps (Fig. 5 H, closed black circles). However, the much shallower increases in $K_{0.5}$(Ko) at 125 mM [Nao] over the same negative potential range for both RD and C113Y pumps with C-terminal deletions (Fig. 5, I and J, closed circles) reveal that those truncations specifically attenuate the steeply voltage-dependent inhibitory Nao binding.

Influence of Nao and C-terminal truncations on outward Na/K pump currents

The latter effect can be seen more straightforwardly by directly comparing the shapes of ouabain-sensitive, maximally activated (15 mM Ko) Na/K exchange outward current–voltage relationships determined with and without Nao for each C-terminally truncated mutant and each parent construct (Fig. 6, A–D). For WT, C113Y, and RD pumps, the difference between outward Na/K pump currents in Nao-free versus 125-mM [Nao] solutions increased markedly as membrane potential became progressively more negative than −100 mV (Fig. 3 D, open vs. closed symbols). But, in the C-terminally truncated pumps, this Nao-free versus 125-mM [Nao] difference was much smaller than in the parent pumps. Thus, the Nao-dependent difference for C113Y-ΔKESYY pumps (Fig. 6 A, open vs. closed blue squares) and C113Y-ΔYY pumps (Fig. 6 B, open vs. closed olive squares) was about half that for the parent C113Y pumps (Fig. 6, A and B, open vs. closed red squares). For RD-ΔKESYY (Fig. 6 C, open vs. closed magenta squares) and RD-ΔYY (Fig. 6 D, open vs. closed orange squares) pumps, the Nao-free versus 125-mM [Nao] difference was less than half that for the parent RD pumps (Fig. 6, C and D, open vs. closed green squares). This diminished impact on outward Na/K pump current–voltage relationships of switching from Nao-free to Nao-containing solution is further evidence that the C-terminal truncations weaken the influence of Nao on forward Na/K cycling at large negative potentials.

Maximal turnover rates of Na/K pumps are little influenced by ΔYY or ΔKESYY truncations

The current–voltage relationships in Fig. 6 (and in Fig. 3 D) are all normalized to their mean amplitude between 0 and 60 mV. If the number (Np) of active

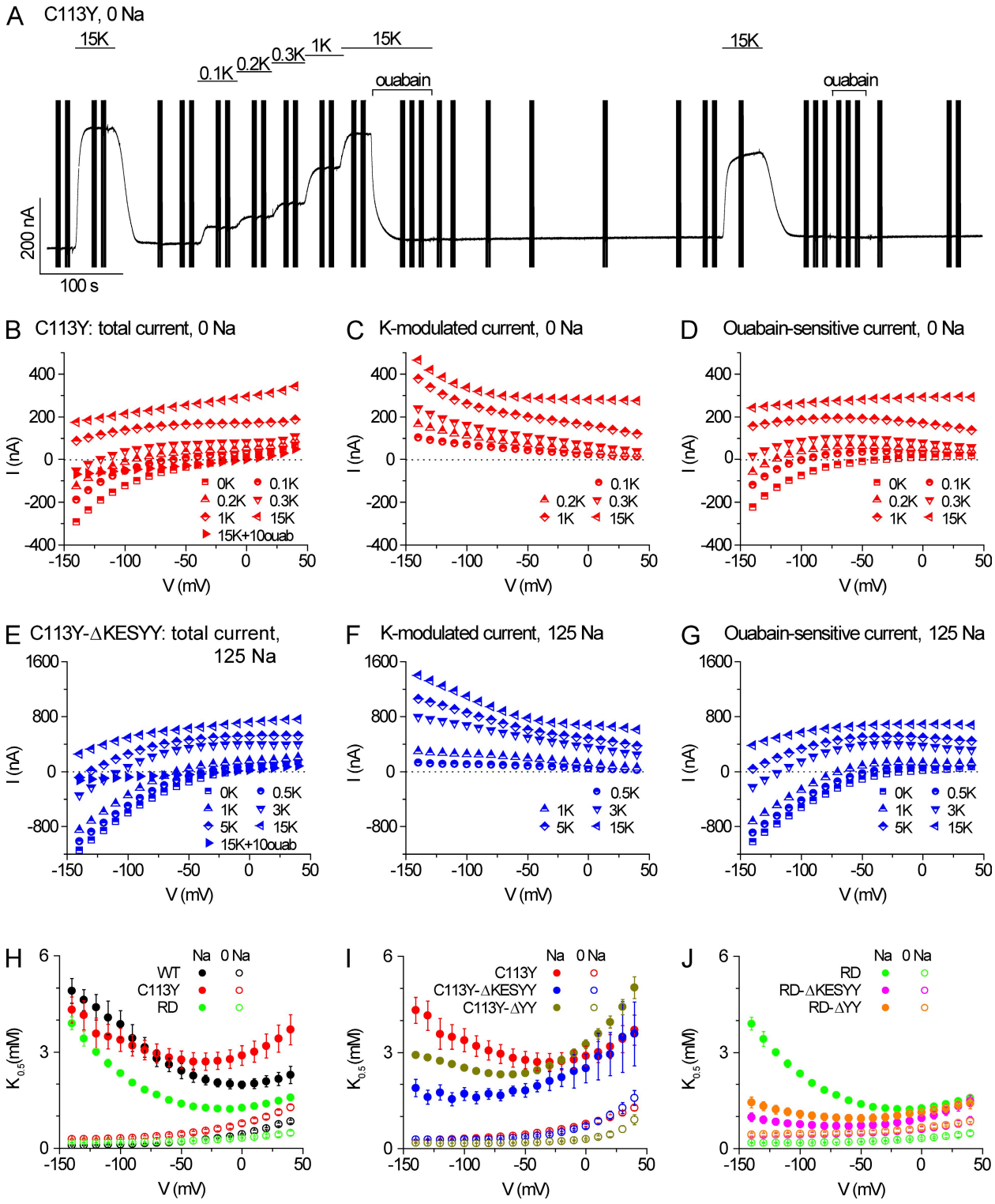

Figure 5. Ko sensitivity of Na/K pump–mediated currents in Nai-loaded oocytes expressing WT or mutant Na/K pumps. (A) Changes in holding current at −50 mV in response to stepwise increments of [Ko] in C113Y Na/K pumps in 0 mM Nao; the vertical lines mark application of 100-ms voltage steps to −140 to 40 mV in 10-mV increments. (B) Steady-state I-V plots at the indicated [Ko] from A. (C and D) Corresponding Ko-modulated I-V plots (C) and ouabain-sensitive I-V plots (D) from data in A and B obtained by appropriate subtraction. (E–G) Analogous I-V plots to those in B–D, but for C113Y-ΔKESYY Na/K pumps in 125 mM Nao. (H–J) Hill fits to the Ko-modulated steady currents at the various [Ko] at each voltage yielded the mean $K_{0.5}$(Ko) values for each pump type in the absence (open circles) or presence (closed circles) of Nao (WT, black; C113Y, red; RD, green; C113Y-ΔKESYY, blue; C113Y-ΔYY, olive; RD-ΔKESYY, magenta; RD-ΔYY, orange). Error bars represent SEM.

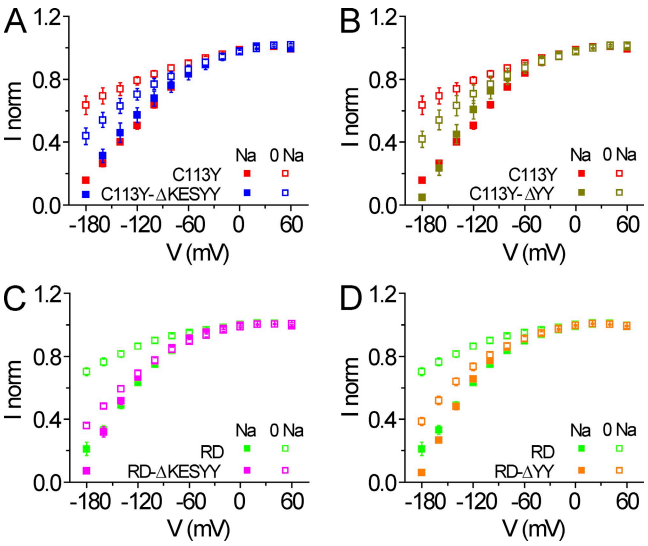

Figure 6. Diminished difference between 125 mM and 0 mM Nao at large negative potentials in ΔYY and ΔKESYY truncated Na/K pumps. (A–D) Mean ouabain-sensitive outward Na/K pump currents (normalized as in Fig. 3 D; mean ± SEM of 6–12 oocytes from at least two frogs) at 15 mM [Ko] and 0 mM Nao (open squares) or 125 mM Nao (closed squares) for ΔKESYY (A and C) and ΔYY (B and D) truncated pumps are shown superimposed on the corresponding I-V plots for the parent C113Y (A and B) and RD (C and D) pumps: (A) C113Y (red) and C113Y-ΔKESYY (blue); (B) C113Y (red) and C113Y-ΔYY (olive); (C) RD (green) and RD-ΔKESYY (magenta); (D) RD (green) and RD-ΔYY (orange). Error bars represent SEM.

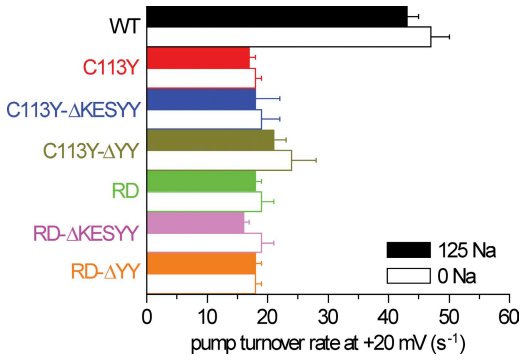

Figure 7. Summary of maximal Na/K pump turnover rates at 22–24°C estimated by normalizing ouabain-sensitive Na/K pump currents at 20 mV and 15 mM [Ko] obtained with or without Nao to the total ouabain-sensitive charge moved between voltage extremes in the same oocyte in a Ko-free 125-mM Nao solution (e.g., Fig. 8, D and H) taken as a measure of the number of Na/K pumps in the membrane. With Nao, closed bars; without Nao, open bars. The estimates assume 3Na:2K stoichiometry during pumping and the pre–steady-state movement at 0 mM [Ko] of z_q net charges (for WT, $z_q = 0.93 \pm 0.03$; for RD and C113Y pumps with or without C-terminal truncations, mean $z_q = 0.65 \pm 0.01$; values taken from Fig. 9, A and B) across the electric field of the membrane between extreme positive and negative potentials; unless these parameters differ between pump types, the estimates are expected to be proportional to true turnover rates. Estimated rates for WT pumps (black) are at least twice those for all other pumps, regardless of the presence or absence of Nao or of C-terminal truncations. Rate estimates in the presence and absence of Nao, respectively, averaged as follows: WT, $43 \pm 2\ s^{-1}$ and $47 \pm 3\ s^{-1}$, $n = 5$; C113Y (red), $17 \pm 1\ s^{-1}$ and $18 \pm 1\ s^{-1}$, $n = 7$; C113Y-ΔKESYY (blue), $18 \pm 4\ s^{-1}$ and $19 \pm 3\ s^{-1}$, $n = 8$; C113Y-ΔYY (olive), $21 \pm 2\ s^{-1}$ and $24 \pm 4\ s^{-1}$, $n = 5$; RD (green), $18 \pm 1\ s^{-1}$ and $19 \pm 2\ s^{-1}$, $n = 5$; RD-ΔKESYY (magenta), $16 \pm 1\ s^{-1}$ and $19 \pm 2\ s^{-1}$, $n = 8$; RD-ΔYY (orange), $18 \pm 1\ s^{-1}$ and $18 \pm 1\ s^{-1}$, $n = 3$. Error bars represent SEM.

Na/K pumps in each oocyte were known, then, assuming constant 3Na:2K transport stoichiometry and thus extrusion of one elementary charge (e) per turnover, the mean maximal turnover rate (kmax) could be calculated from the maximal outward Na/K pump current in each oocyte (Ip,max; obtained as ouabain-sensitive current at 15 mM [Ko] and 20 mV) from the relation $kmax = Ip,max/(Np \times e)$. An estimate for Np can be found from the total transient charge movement (Q_{tot}) mediated by the same population of pumps under noncycling Na/Na exchange conditions (see the following paragraph) and the voltage sensitivity of that charge movement, which provides a measure of the charge moved per pump ($z_q \times e$); then $Np = Q_{tot}/(z_q \times e)$. Maximal turnover rates were thus estimated as $kmax = (Ip,max \times z_q)/Q_{tot}$ for each pump type (Fig. 7). The turnover rate was ~50 s^{-1} for WT Na/K pumps with or without Nao and roughly twofold lower on average for C113Y and RD pumps, regardless of the presence or absence of Nao or of either C-terminal truncation. The similarity of the turnover rates for all our C113Y and RD pumps (Fig. 7) justifies the normalization used for the comparisons made in Fig. 6.

Nao-dependent transient charge movements probe voltage-dependent Nao binding

We further examined the influence of the C-terminal truncations on pump interactions with Nao by assessing the characteristics of pump-mediated transient charge movement induced by voltage jumps (Fig. 2 A) in the presence of 125 mM [Nao] but in the absence of Ko (e.g., Nakao and Gadsby, 1986; Rakowski, 1993). Representative superimposed currents for C113Y pumps without (Fig. 8 A) and with (Fig. 8 B) 10 mM ouabain and the ouabain-sensitive currents obtained by subtraction (Fig. 8 C) confirm the absence of steady-state pump-mediated current (and thus of stationary electrogenic cycling) at all voltages (compare with Fig. 2 E). The ouabain-sensitive records also reveal transient currents with approximately exponential decay time courses (Fig. 8 C, red fit lines) that are slower during steps to more positive potentials and faster at more negative potentials. The time constant range, 1–4 ms (Figs. 8 C and 9 C), identifies these charge movements as the slowest of the three components observed in WT Na/K pumps under similar conditions in preparations affording higher time resolution (Hilgemann, 1994; Wuddel and Apell, 1995; Holmgren et al., 2000). The quantities of charge moved, which were obtained by direct integration of the transient currents, were closely similar during (Fig. 8 D, ON) and after (Fig. 8 D, OFF) each test

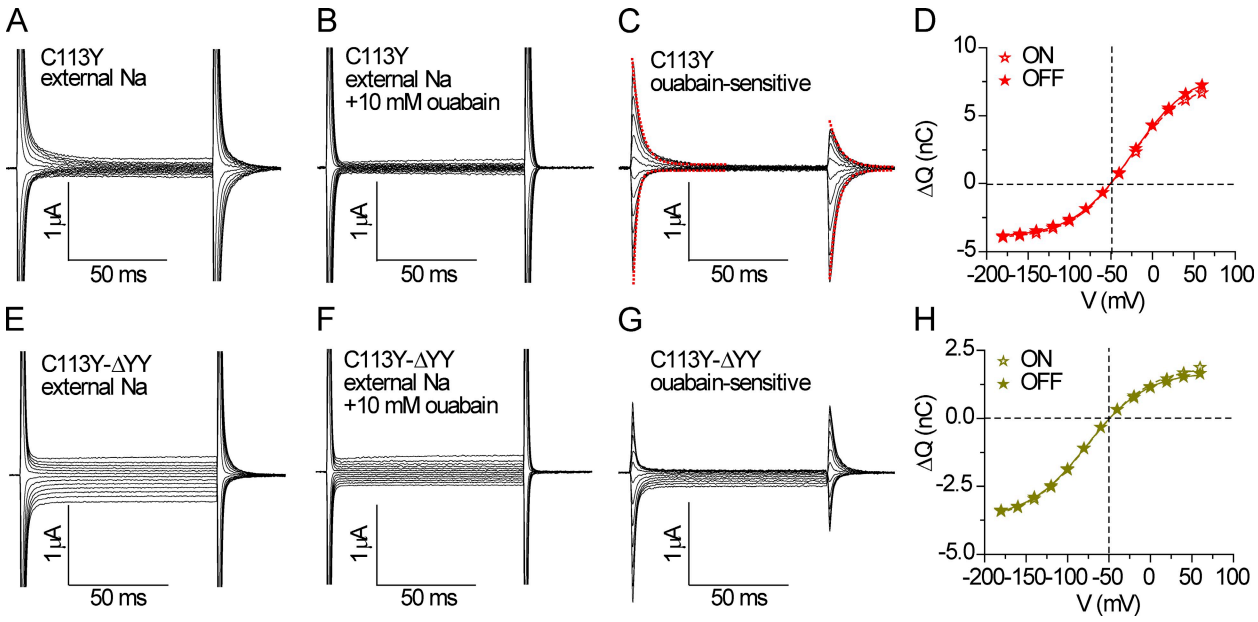

Figure 8. Representative ouabain-sensitive pre–steady-state currents under Na/Na exchange conditions for C113Y and C113Y-ΔYY pumps. (A–D) C113Y pumps; (E–H) C113Y-ΔYY pumps. Superimposed current records obtained in 125 mM Nao before (A, C113Y; E, C113Y-ΔYY) and after (B, C113Y; F, C113Y-ΔYY) adding 10 mM ouabain. Ouabain-sensitive transient currents determined by direct subtraction of the records in A and B and in E and F, respectively, are shown in C for C113Y and in G for C113Y-ΔYY Na/K pumps (red lines in C show single exponential fits to ON and OFF transient currents elicited by steps to 60 mV and −180 mV for relaxation rate estimates of Fig. 9 [C and D]). Pre–steady-state charge was obtained directly as the time integral of the transient currents (C and G) at the ON and OFF voltage steps after baseline subtraction of any steady current. (D and H) The charge–voltage distributions were fit with the Boltzmann relation

$$Q(V) = Q_{max} + \frac{(Q_{min} - Q_{max})}{1 + e^{\left[z_q F(V - V_{0.5})/RT\right]}},$$

where V is the test voltage, Q_{min} and Q_{max} are the charge moved for extreme negative and positive voltage steps, z_q is the effective charge, $V_{0.5}$ is the midpoint voltage, and F, R, and T have their usual meaning. ON and OFF values are, respectively, for D as follows: Q_{min}, −4.0 nC and −3.9 nC; Q_{max}, 7.5 nC and 8.2 nC; z_q, 0.74 and 0.71; $V_{0.5}$, −29 mV and −25 mV. ON and OFF values are, respectively, for H as follows: Q_{min}, −3.8 nC and −3.7 nC; Q_{max}, 1.9 nC and 1.7 nC; z_q, 0.66 and 0.69; $V_{0.5}$, −74 mV and −77 mV.

voltage step, and their voltage dependence was well described by Boltzmann relations.

In contrast, the C-terminally truncated pumps all generated steady-state ouabain-sensitive current in 125-mM [Nao], 0-mM Ko solution (Figs. 4 and 5 G). This steady current was small and inward near the −50-mV holding potential, became larger in amplitude at progressively more negative potentials, and was relatively small and outward at positive potentials (Fig. 5, E and G, 0 mM Ko). However, as that current appeared to be time independent (e.g., C113Y-ΔYY; Fig. 8, E–G), it was assumed to not contribute to OFF charge movement after steps back from test voltages (Fig. 8 G), and ON charge movement could still be obtained by integrating pre–steady-state current at each test voltage. As exemplified by C113Y-ΔYY (Fig. 8 H), for each voltage jump, these ON and OFF transient charge movements were equivalent. More than half the total charge was moved during jumps to voltages more positive than the −50-mV holding potential for C113Y pumps (Fig. 8, C and D) but during jumps to potentials more negative than −50 mV for C113Y-ΔYY (Fig. 8, G and H). This means that the midpoint of the charge–voltage curve lies positive to −50 mV in C113Y pumps but negative to −50 mV in C113Y-ΔYY pumps, reflecting a leftward shift of the charge–voltage curve in the latter pumps (Fig. 9 A). That shift amounted to ∼50 mV for ΔYY truncations (compare with Fig. 8, D and H) and ∼70 mV for ΔKESYY truncations and was similar in C113Y (Fig. 9 A) and RD (Fig. 9 B) pumps. Such a leftward shift means that stronger negative voltages were required to drive the E1P(Na3) ↔ E2P3Na equilibrium (Fig. 1 B, left) toward E1P(Na3), as if that Na-occluded state were relatively less stable in pumps with C-terminal deletions.

Similar leftward shifts of charge–voltage curves for the slow component of transient charge have previously been observed in WT Na/K pumps upon lowering [Nao] (Gadsby et al., 1992; Rakowski, 1993; Hilgemann, 1994; Holmgren et al., 2000) and are shown here for C113Y pumps (Fig. 10, A–D) and for C113Y-ΔYY pumps (Fig. 10, E–H) in response to two- and eightfold reductions in [Nao] from the usual 125 mM (Fig. 10, D and H). These leftward shifts are likewise interpreted as reflecting reduced occupancy at the lower [Nao] of the Na-bound

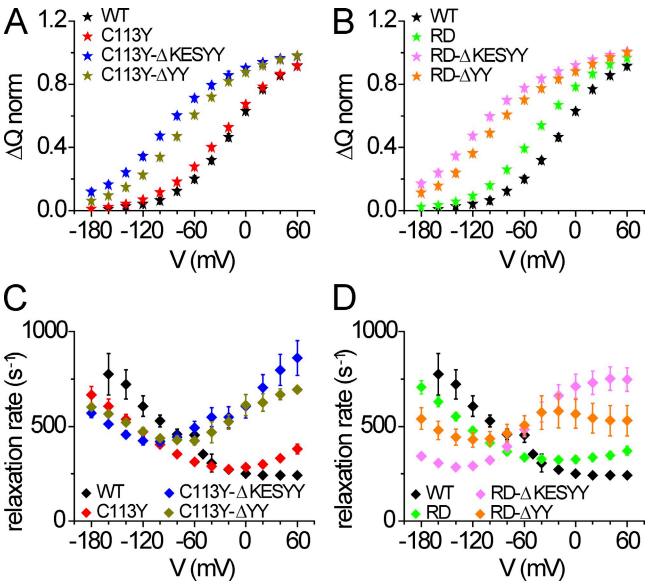

Figure 9. ΔYY and ΔKESYY truncations shift ouabain-sensitive transient charge movements to more negative potentials and accelerate charge relaxation at positive potentials. (A and B) Charge–voltage distributions determined from OFF voltage steps (as for closed symbols in Fig. 8 [D and H]) were normalized by their estimated amplitude from fits (Q_{max}–Q_{min}, 12.1 nC and 5.4 nC, respectively, for Fig. 8 [D and H]) and were averaged. $V_{0.5}$ and z_q values for each pump type averaged as follows: WT (black), −16 ± 1 mV and 0.93 ± 0.03, n = 3; C113Y (red), −26 ± 1 mV and 0.70 ± 0.01, n = 13; RD (green), −44 ± 1 mV and 0.74 ± 0.02, n = 12; C113Y-ΔKESYY (blue), −96 ± 2 mV and 0.62 ± 0.05, n = 7; C113Y-ΔYY (olive), −75 ± 1 mV and 0.67 ± 0.01, n = 5; RD-ΔKESYY (magenta), −114 ± 2 mV and 0.59 ± 0.02, n = 11; RD-ΔYY (orange), −95 ± 2 mV and 0.60 ± 0.02, n = 5. (C and D) Single exponential fits to the decay time courses of the transient current elicited by the ON voltage steps (e.g., Fig. 8 C, red lines) gave relaxation rates of the slow components of charge movement; their mean values are plotted against voltage in C and D. Error bars represent SEM.

state E2P3Na and, via the E1P(Na3) ↔ E2P3Na equilibrium, also of E1P(Na3) at a given voltage. This reduced occupancy of conformations with three bound Na can be overcome by stronger negative voltages as a result of the steeply voltage-dependent binding of the third Nao ion. For the simplest access channel models (Gadsby et al., 1993; Rakowski, 1993; Heyse et al., 1994; Hilgemann, 1994; Holmgren et al., 2000; De Weer et al., 2001), the midpoint shifts ($\Delta V_{0.5}$) yield estimates of the fraction of the membrane's electric field (λ) traversed by Nao ions in reaching their binding site through $\Delta V_{0.5} = (RT/\lambda F) \ln([Nao]_1/[Nao]_2)$. The shifts observed here give λ values of 0.73 for C113Y (Fig. 10 D) and 0.65 for C113Y-ΔYY (Fig. 10 H), comparable with those of ∼0.7 previously found for WT Na/K pumps by comparable measurements (Rakowski, 1993; Heyse et al., 1994; Hilgemann, 1994; Wuddel and Apell, 1995; Holmgren et al., 2000).

Although for simplicity, OFF charge amounts are plotted in Fig. 10 (D and H), we found that ON and OFF pre–steady-state charge movements were similar under all conditions (Fig. 8 H), even in the presence of large inward currents at the lowest [Nao] (Fig. 10 G). The slower relaxation time courses at the most negative potentials as [Nao] is lowered (Fig. 10, E–G) reflect the leftward shifts of the rate–voltage curves in parallel with charge–voltage curves expected from observations on WT Na/K pumps (Gadsby et al., 1992; Rakowski, 1993; Hilgemann, 1994; Holmgren et al., 2000; Holmgren and Rakowski, 2006).

Influence of C-terminal truncations on voltage-dependent equilibration rates

In addition, those C-terminal truncations had striking effects on equilibration rates and how they varied with test potential. In the control WT, C113Y, and RD pumps, the relaxation rates of the transient currents progressively increased as test potentials were made more negative and were generally lower at positive potentials (Fig. 9, C and D). In all of the C-terminally truncated pumps, however, the relaxation rates were increased at positive voltages, and, especially for RD-ΔYY and RD-ΔKESYY pumps, the increase in relaxation rates at negative potentials seemed displaced to larger negative voltages (Fig. 9, C and D). These kinetic changes are also consistent with relative destabilization of the occluded E1P(Na3) state (see Discussion section C-terminal truncations...).

Influence of C-terminal truncations on interactions with Ko ions

If C-terminal truncations impair the ability of Na/K pumps to stably occlude Na ions, as the data presented so far imply, might occlusion of K ions also be affected? Maximal turnover rates, determined at saturating [Ko] from either steady-state Na/K pump currents (Fig. 7) or ATPase rates (Toustrup-Jensen et al., 2009), are not altered by the truncations, which suggests that they do not affect the rate-limiting step in the transport cycle. If the cycle is rate limited by the ATP binding–mediated conformational change, E2(K2)-ATP → E1-2K-ATP, which releases K to the cytoplasmic side (Fig. 1 B, right), this would imply that the energetics of that step are independent of C-terminal contacts. At the extracellular side, the energetics of occlusion and deocclusion of Ko ions have been studied far less than those of Nao ions. One reason is that the weakly voltage-dependent binding of Ko to the electrically shallow extracellular sites gives rise to charge movements so small and rapid that their characterization has required lowered temperature and use of the K congener Tl to slow them (Peluffo and Berlin, 1997). However, we have previously reported the robust modulation of the gating of palytoxin-bound Na/K pump channels by Ko ions: in the absence of cytoplasmic nucleotides, sudden replacement of all Nao with Ko quickly shut palytoxin-bound pump channels (Artigas and Gadsby, 2003). The rapid reduction of pump channel current was interpreted to reflect stabilization of the closed conformation

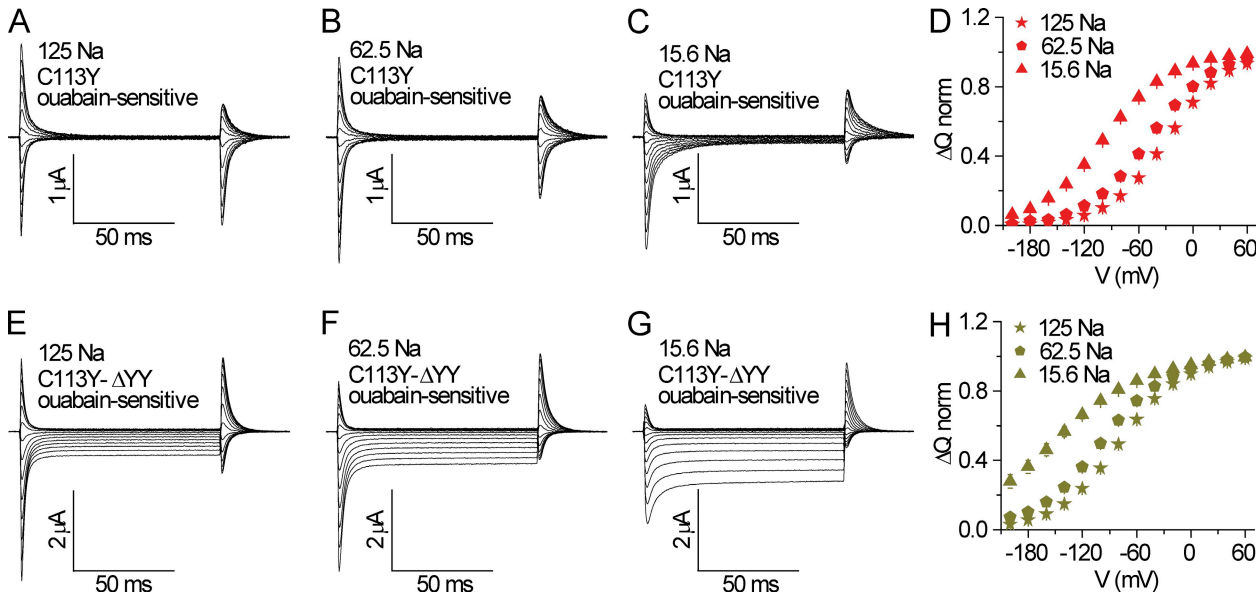

Figure 10. Similar Nao dependence and voltage dependence of transient charge movements in parent C113Y pumps and in C113Y pumps with C-terminal truncations. (A–C) Superimposed ouabain-sensitive current records (obtained by subtraction as in Fig. 8 [C and G]) determined in the same oocyte for C113Y pumps exposed to 125 mM (A), 62.5 mM (B), and 15.6 mM (C) [Nao]; Na was replaced by equimolar TMA. (E–G) Similar ouabain-sensitive transient currents in an oocyte expressing C113Y-ΔYY pumps exposed to 125 mM (E), 62.5 mM (F), and 15.6 mM (G) [Nao]; note that the steady inward currents at negative test voltages became larger as [Nao] was lowered (E–G). (D and H) Pre–steady-state charge determined as integrals of OFF transients was plotted against test voltage and fitted with Boltzmann relations and then normalized and averaged for four C113Y oocytes (D) and three C113Y-ΔYY oocytes (H). $\Delta V_{0.5}$ for the twofold and eightfold reductions of [Nao], respectively, averaged as follows: C113Y (red), −22 ± 1 mV and −80 ± 3 mV, $n = 4$; C113Y-ΔYY (olive), −25 ± 2 mV and −90 ± 10 mV, $n = 3$; C113Y-ΔKESYY, −33 mV and −102 mV, $n = 1$. Fractional electrical distance, λ, estimated from these data via $\Delta V_{0.5} = (RT/\lambda F)\ln([Nao]_1/[Nao]_2)$ is ∼0.7 (0.73 for C113Y and 0.65 for C113Y-ΔKESYY), as for WT.

of the extracellular gate after binding of Ko ions (compare with Fig. 1 B). We therefore deemed this a suitable system for testing whether the C-terminal truncations influence occlusion of Ko ions.

We first tested whether the C-terminal truncations affected the ability of palytoxin to transform Na/K pumps into channels (Fig. 11, A and B). With symmetrical 125-mM [Na] solutions and no cytoplasmic-side (pipette) ATP, exposure of excised outside-out patches at −50 mV to a high concentration (100 nM) of palytoxin promptly activated inward currents in WT, C113Y (Fig. 11 A), and RD Na/K pumps; the time courses were all reasonably well approximated by single exponentials with similar time constants of 20–40 s (Fig. S3 A). In the pumps with C-terminal truncations, the time courses of palytoxin-induced current activation were no different (e.g., C113Y-ΔYY; Fig. 11 B and Fig. S3 A).

As previously described for WT pumps, in patches containing C113Y or RD pump channels, sudden replacement of all Nao with Ko initiated three phases of changes in the inward current (Artigas and Gadsby, 2003). First, there was an instantaneous few-percent increase (Fig. 11 A, asterisk) as a result of the more rapid permeation of Ko than Nao ions through open pump channels (Artigas and Gadsby, 2004). The increase was immediately followed by a large current decrease with fast and slow components of current decay (Fig. 11, A and C) interpreted to reflect, respectively, reduction of the open probability of the extracellular-facing gate followed by unbinding of palytoxin (Artigas and Gadsby, 2003). These three phases of current change, small rapid increase followed by fast and slow current decreases, were also seen in the C113Y and RD pumps with C-terminal deletions (e.g., C113Y-ΔYY; Fig. 11 B). However, in the C-terminally truncated pumps, the fraction of the current that decayed rapidly on switching from Nao to Ko was consistently smaller (∼45–50%; Fig. 11, B and C; and Fig. S3 B) than in WT or in the C113Y or RD parent pumps (∼70–80%; Fig. 11, A and C; and Fig. S3 B). In addition, the resulting larger slow fraction of the current decline in the truncated pumps decayed somewhat more slowly than that in the parent pumps (Fig. 11, A–C). These results demonstrate that the C-terminal truncations make it harder for Ko ions to shut palytoxin-bound pump channels. The truncations cause a shift in the equilibrium of the extracellular-facing gate that would be equivalent to destabilization of the occluded K conformation, E2(K2), in the absence of palytoxin.

DISCUSSION

Evaluation of ouabain-resistant background Na/K pump constructs

Functional experiments of Na/K pump mutations in animal cells require their introduction into ouabain-resistant

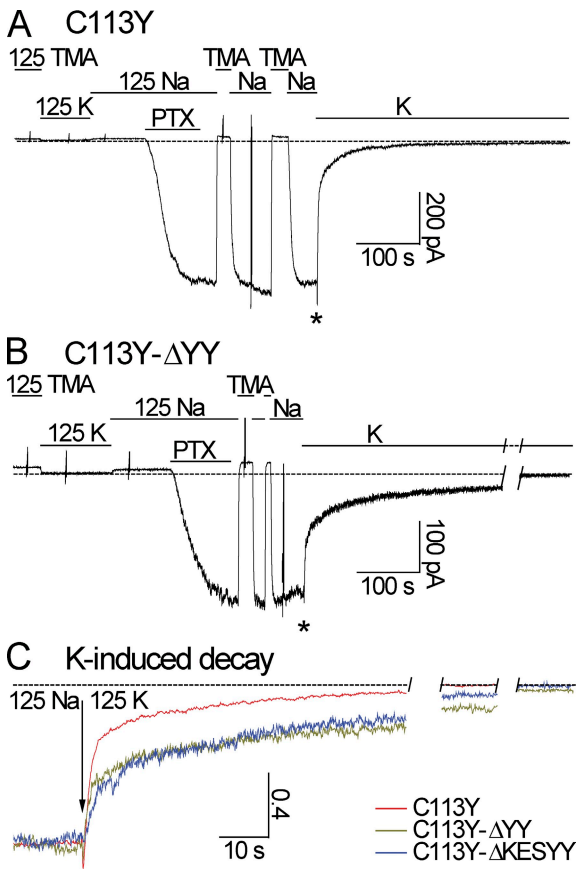

Figure 11. ΔYY and ΔKESYY C-terminal truncations impair Ko-induced closure of palytoxin-bound Na/K pump channels. (A and B) Representative recordings of activation and deactivation of palytoxin-bound Na/K pump channels in outside-out membrane patches (with 125 mM Na but no ATP in the pipette–cytoplasmic side) excised from oocytes expressing C113Y (A) or C113Y-ΔYY truncated (B) pumps; the labeled bars indicate bath (extracellular side) solution changes. A high concentration, 100 nM, of palytoxin (PTX) rapidly opened pump channels in both cases with similar time courses (activation time constant, τ_{act} = 21 s for C113Y and 26 s for C113Y-ΔYY). Replacement of all Nao with Ko caused, after a small instantaneous current increase (asterisks), biexponential complete decay of palytoxin-activated current (dotted lines mark current levels in Ko before PTX). (C) Superimposed normalized traces show reduced fractional amplitude of the faster component of Ko-induced decay for the truncated pumps (C113Y-ΔYY, olive; C113Y-ΔKESYY, blue) than for the parent pump (C113Y, red); dotted line as in A and B; breaks in the traces are to show that the decay is complete.

Na/K pumps. This allows inclusion in all solutions of a low concentration of ouabain, sufficient to prevent contributions from endogenous, ouabain-sensitive Na/K pumps so that effects of the introduced mutations can be isolated. To be certain of the molecular composition of the ouabain-resistant Na/K pumps that we study after expressing them in *Xenopus* oocytes, we lowered the ouabain sensitivity of *Xenopus* α1 subunits by point mutation and coexpressed them with native *Xenopus* β3 subunits to yield ouabain-resistant *Xenopus* α1β3 Na/K pumps. We diminished ouabain sensitivity by either the paired substitutions Q120R/N131D (called RD) to mimic the homologous residues in naturally ouabain-resistant rat Na/K pump α1 subunits (Price and Lingrel, 1988) or the point mutation C113Y (Canessa et al., 1992). The resulting RD Na/K pumps were half-maximally inhibited by ~200 µM ouabain and the C113Y Na/K pumps by ~25 µM ouabain, which allowed endogenous pumps to be silenced by the continuous presence of 1 µM ouabain and mutant pump function to then be isolated as that abolished by 10 mM ouabain.

As the RD mutations (in the TM1–TM2 loop) alter charge near the extracellular ion entryway and the C113Y mutation occurs within TM1, part of the TM1–TM2 helical hairpin unit that moves substantially during the Na/K pump cycle, it is not surprising that some differences could be discerned between WT and ouabain-resistant RD or C113Y pumps. Two differences were striking. First, the maximal turnover rates of RD and C113Y pumps were approximately twofold lower than that of WT (Fig. 7). Intrigued to know whether rat α1 Na/K pumps would be similarly slow, we expressed rat α1 Na,K-ATPase (plus *Xenopus* β3) in the oocytes and performed the same measurements of maximally activated outward Na/K pump current and of transient Na charge movements in Ko-free solution as for all the other pumps. The estimated turnover rates for the rat pumps were 16 ± 1 s^{-1} in 125 mM [Nao] and 18 ± 1 s^{-1} in 0 mM Nao (n = 6; not depicted), which is closely similar to those for RD *Xenopus* pumps (Fig. 7). These rates of around 20 s^{-1} for RD *Xenopus* pumps and rat pumps at 22–24°C, calculated from pump currents, agree reasonably well with the ATP hydrolysis rate of ~140 s^{-1} determined at 37°C for rat α1 Na,K-ATPase (Toustrup-Jensen et al., 2009); the latter rate was also unaffected by comparable C-terminal truncations to those tested here (compare with Fig. 7). The second difference was that, unlike WT, in Ko- and Nao-free solutions at pH 7.6, RD and C113Y pumps displayed an ouabain-sensitive steady-state inward current that increased steeply with voltage at negative potentials. This substantial inward current was not evident in WT pumps under those conditions, but it resembles the large and similarly voltage-dependent current previously reported in WT pumps at low pH (Efthymiadis et al., 1993) and ascribed to dissipative proton flow through an E2P-like conformation of the Na/K pump (Wang and Horisberger, 1995; Vasilyev et al., 2004) possibly somehow related to binding of the third Na ion (Li et al., 2006).

Possible origins of the inward current in Ko-free solutions

Although learning the mechanism of these inwardly rectifying pump-mediated currents was not the goal of this study, we needed to characterize those currents well enough to eliminate their contribution to the pump current signals of interest. First, we compared inward current amplitude at −180 mV and at 0 mM [Ko] without and with 125 mM [Nao] for each construct because

the inward current proposed to be carried by protons in WT pumps in Ko- and Nao-free solution at low pH is strongly diminished by ≥100 mM [Nao] (Efthymiadis et al., 1993; Wang and Horisberger, 1995; Vasilyev et al., 2004). We found that, similarly, the inward current in the parent RD and C113Y pumps in Ko- and Nao-free solution, but at pH 7.6, was greatly reduced by 125 mM [Nao] (Fig. 4). However, the inward currents observed in the C-terminally truncated C113Y pumps were similarly large in the presence or absence of Nao (Fig. 4). In contrast, in the C-terminally truncated RD pumps, these inward currents were large in the presence of Nao but were much smaller in its absence (Fig. 4). The latter scaling of inward current amplitude with [Nao] in truncated RD pumps was recently interpreted as indicating that Nao ions carried the inward current (Yaragatupalli et al., 2009; Meier et al., 2010). However, this seems unlikely because the presence or absence of Nao had little effect on the large inward current in C113Y truncated pumps (indeed, in C113Y-ΔYY pumps, it was even larger without Nao; Figs. 4 and 10, E–G), and in both RD and C113Y parent pumps, exposure to 125 mM [Nao] nearly abolished the current (Fig. 4).

A clue to understanding these disparate effects of Nao may be found in the consistently inhibitory action of Ko on the inward currents (Fig. 2, B–E; and Fig. 5), which occurs with the same $K_{0.5}$(Ko) for activation of outward Na/K pump current. The simplest explanation is that Ko binding to E2P states alters the steady-state distribution of pump conformations (toward the right side of Fig. 1 B) such that occupancy of states that support cyclic Na/K exchange is favored at the expense of the states that underlie the inward current (compare with Wang and Horisberger, 1995; Meier et al., 2010). By the same token, whether addition of Nao increases, decreases, or leaves unchanged the inward current observed in its absence can be explained in terms of alterations of the steady-state occupancy of the conformations involved in generating the inward current; the different directions of the changes could be accounted for by differences in the initial distributions of states for the various mutant pumps and in their apparent affinities for Nao. The known relatively low apparent affinities of Nao interactions with E2P-related Na/K pump states could result in alterations that vary approximately linearly with [Nao] (Yaragatupalli et al., 2009), inviting the interpretation that they reflect changes in the concentration of the current-carrying ion (Yaragatupalli et al., 2009; Meier et al., 2010). However, all observations to date on modulation of these inward currents through Na/K pumps can be explained by ion binding–induced redistributions of pump conformations, with protons being the sole current carrier.

So how might the inward currents be generated? As previously noted (Yaragatupalli et al., 2009; Meier et al., 2010), the largest inward currents at −180 mV are only approximately three times larger than the maximally activated outward Na/K exchange currents generated by the same populations of pumps in the same oocytes (Fig. 2, C and E; and Fig. 4). Because those outward currents correspond to turnover rate estimates of ∼40 s^{-1} (Fig. 7), the inward currents reflect flow across the membrane of only ∼100 ions s^{-1} per pump on average. This is approximately five orders of magnitude slower than Na or K ion flow through palytoxin-bound Na/K pump channels (Artigas and Gadsby, 2003). In addition, the inward current of RD-ΔYY pumps has been shown to have a high enthalpic activation energy >100 kJ/mol, like that of outward Na/K exchange current of the same pumps, implying that the inward current is similarly rate limited by substantial conformational change (Meier et al., 2010; compare with Rettinger, 1996). Together, these results admit two alternative explanations. One possibility is that the inward current flows through an ion channel–like conformation of the pump with vanishingly small open probability and/or unitary conductance and gating that involves major conformational changes. This is compatible with the low ion throughput rate and high activation energy and possibly even with the tendency toward current saturation at high [Nao] and extreme negative potentials hinted at by the data of Meier et al. (2010). However, it seems more likely that an E2P-related state (or pair of adjacent states) alternately exposes a protonatable side chain to the extracellular access channel and then to the cytoplasmic-side access pathway. Just such a current mechanism has been shown to result from introduction of a single histidine residue at strategic locations on the voltage sensor of a voltage-gated K channel, which gives rise to voltage-sensitive proton currents whose magnitude varies with the pH gradient across the membrane (Starace and Bezanilla, 2004).

Which states of the pump might be involved? The three relaxation phases of transient currents after deocclusion or binding of Nao in Na/K pumps signal the presence of at least three conformations with one or more bound Na ions along that kinetic pathway. The fact that the inward current is larger in low, 5–25 mM [Nao] than in Nao-free solution or in higher [Nao] (Efthymiadis et al., 1993; Wang and Horisberger, 1995) suggests that one or more of those conformations, perhaps with only one or two bound Na ions, might be likely candidates. Which protonatable side chains might be involved? Among other possibilities, several carboxylates help to coordinate transported Na and K ions in the binding pockets and thus may be expected to change their accessibility between E1 and E2 major conformations. Indeed, fluorescence measurements on Na/K pumps suggest that two protons can occupy the two cation-binding sites alternately shared by Na and K ions (Apell and Diller, 2002). Therefore, reasonable candidates for involvement would be the subset of cation-coordinating

carboxylates closest to pathways accessible to protons from both sides of the membrane in E2P-like structures containing one or two Na ions. However, because there is presently no high resolution structure of any Na-bound Na/K pump conformation, we cannot yet specify the most likely candidates. Of course, if a Na-coordinating carboxylate were involved in shuttling protons, as we suggest, that might help explain some of the observed complexity of Nao and pHo effects on the inward current (Fig. 4; Efthymiadis et al., 1993; Wang and Horisberger, 1995; Vasilyev et al., 2004; Yaragatupalli et al., 2009; Meier et al., 2010).

C-terminal truncations weaken voltage-dependent interactions with Nao

Evidence from steady-state Na/K pump current–voltage relationships. Our measurements of the sensitivity of membrane currents to a range of [Ko] (Fig. 5) and of [ouabain] (Fig. S2) showed that, for all of the pumps, 15 mM [Ko] was a sufficient concentration to fully activate outward Na/K exchange current and fully inhibit inward current in the absence of Nao and to almost completely (≥80%) activate outward current and inhibit inward current in 125 mM [Nao]; they also showed that 10 mM ouabain abolished all pump-mediated current. We can therefore be confident that the maximally activated Na/K pump current–voltage relationships determined, as ouabain-sensitive currents at 15 mM [Ko], in the absence of Nao (Fig. 6, open symbols) are accurate and uncontaminated by any inward current. Overlaying these normalized relationships obtained without Nao on those obtained in the presence of Nao directly reveals the influence of Nao. For the parent C113Y (Fig. 6, A and B) or RD (Fig. 6, C and D) pumps, this influence, apparent as the difference between the Na/K pump current–voltage curves with and without Nao, was greatest at large negative potentials. That difference was diminished for the truncated ΔYY and ΔKESYY pumps and was smallest in the C-terminally truncated RD pumps (Fig. 6, C and D).

Moreover, the conclusion that the influence of Nao was diminished in the ΔYY and ΔKESYY pumps could only be strengthened by any correction of the Na/K pump currents obtained in 125 mM [Nao] to account for incomplete activation of outward Na/K exchange current and incomplete abolition of inward current by 15 mM [Ko]. From the $K_{0.5}$(Ko) values (Fig. 5) and inward/outward current ratios (Fig. 4), we estimate that such corrections would slightly augment Na/K pump currents in Nao (Fig. 6, closed symbols) at large negative potentials: the increase would be by ≤20% for the parent C113Y or RD pumps (whose inward currents are very small in Nao; Fig. 4) and up to twice that amount for the truncated pumps. The weakened influence of Nao on outward Na/K pump currents in C-terminally truncated pumps evident in Fig. 6 would therefore appear even weaker. Because the inhibitory influence of Nao at negative potentials is attributed to slowing of the Na/K exchange cycle by voltage-driven low affinity binding of one or more Na ions deep within the membrane's electric field (Nakao and Gadsby, 1989; Rakowski et al., 1989; Heyse et al., 1994; Sagar and Rakowski, 1994), we conclude that C-terminal truncation weakens that binding.

Evidence from the Ko dependence of Na/K pump currents. The same conclusion can be drawn from examination of the voltage dependence of $K_{0.5}$(Ko) values determined in the presence and absence of Nao for each construct (Fig. 5, H–J). At positive voltages, 125 mM [Nao] causes a similar three- to fourfold increase in $K_{0.5}$(Ko) (reduction in apparent affinity for Ko relative to Nao-free values) in WT or C113Y or RD pumps (Fig. 5 H), which varies little over the 50-mV range of positive potentials tested. Competition between external K and Na ions for the two electrically shallow binding sites in E2P pump conformations (Nakao and Gadsby, 1989; Rakowski et al., 1991; Heyse et al., 1994; Hilgemann, 1994; Jaisser et al., 1994; Berlin and Peluffo, 1997) can account for this invariance. This is because more positive potentials are expected to weaken both inhibitory Nao binding and stimulatory Ko binding in parallel, thus keeping inhibition by Nao approximately constant over the positive potential range. The shallow voltage dependence of Ko binding at these relatively superficial sites is reflected in the small positive slopes of all the $K_{0.5}$(Ko)–voltage plots in the absence of Nao (Fig. 5, H–J, open symbols). At positive potentials, those slopes are somewhat steeper for C113Y pumps (Fig. 5 I) than for RD pumps (Fig. 5 J), both in the presence and absence of Nao, but in neither case are they much altered by the C-terminal truncations. This suggests that the truncations have no large effect on the weakly voltage-sensitive sites where Nao and Ko ions compete for binding.

On the other hand, at negative membrane potentials and with 125 mM [Nao], $K_{0.5}$(Ko) grows steeply with voltage magnitude in WT, C113Y, and RD pumps (Fig. 5 H, closed symbols). These steep negative slopes of the $K_{0.5}$(Ko)–voltage plots reflect ever more effective inhibition at increasingly negative potentials caused by strong voltage-dependent binding of the third external Na ion deep within the electric field (Heyse et al., 1994; Hilgemann, 1994; Wuddel and Apell, 1995; Holmgren et al., 2000; Li et al., 2006). The consequent increasing population of pump states with three bound Na ions progressively precludes binding of Ko (Fig. 1 B). Those steep slopes of the $K_{0.5}$(Ko)–voltage curves in 125 mM [Nao] at negative potentials are greatly attenuated in both RD (Fig. 5 J, closed symbols) and C113Y (Fig. 5 I, closed symbols) pumps with C-terminal truncations. We conclude from these results that C-terminal truncation impairs the voltage-dependent binding of the third external Na ion that severely inhibits Na/K pump turnover

at large negative potentials but not the weakly voltage-dependent competition of two external Na ions for the two sites that bind Ko (compare with Toustrup-Jensen et al., 2009; Meier et al., 2010).

Evidence from voltage jump–induced charge movements. Additional evidence that the C-terminal truncations disrupt the strongly voltage-dependent binding of the third Na ion from the extracellular side comes from analysis of the pump-mediated transient charge movements elicited by voltage steps in the presence of Nao but in the absence of Ko (Figs. 8 and 9). The strictly sequential nature of the three components (rapid, medium speed, and slow) of these transient Na charge movements (Hilgemann, 1994; Wuddel and Apell, 1995; Holmgren et al., 2000) was deduced from the observed loss of the two faster components and concomitant growth of the slow component after longer times spent at negative potentials (Hilgemann, 1994; Holmgren et al., 2000); these relationships among the three components led to the proposal that each one signals binding/release of one of the three Na ions. Further analyses of voltage dependence and [Nao] dependence of rates and amounts of charge moved confirmed that the strongly voltage-dependent low affinity Nao binding occurs at the third site and limits the slow step. This relatively low affinity dependence of the slow component of charge movement on [Nao], the absolute value of its relaxation rate, and its high temperature sensitivity provided evidence that it reports equilibration across the major occlusion–deocclusion step, E1P(Na3) ↔ E2P3Na (Nakao and Gadsby, 1986; Gadsby et al., 1992; Rakowski, 1993; Heyse et al., 1994; Hilgemann, 1994; Wuddel and Apell, 1995; Holmgren et al., 2000). Bulk external Na concentration exerts this voltage-dependent influence not only on the slow component of Na charge movement in Na/K pumps deprived of K ions but also on the transport rates of pump-mediated electroneutral Na/Na exchange, or reverse Na/K exchange, or (as discussed in the preceding paragraph) on the extent of inhibition of forward Na/K exchange. In all of these processes, effects of appropriate changes in membrane potential or of [Nao] were found to be kinetically equivalent, and evaluation of their equivalence suggested that they were all limited by external Na ion binding to a site estimated to lie ∼70% of the electrical distance across the membrane from the extracellular side (Nakao and Gadsby, 1989; Gadsby et al., 1993; Sagar and Rakowski, 1994; Heyse et al., 1994; Wuddel and Apell, 1995; Holmgren et al., 2000; De Weer et al., 2001).

Viewed from this perspective, the leftward shifts of the slow charge–voltage curves of the ΔYY and ΔKESYY pumps relative to those of the parent C113Y and RD pumps (Fig. 9, A and B) argue strongly that the C-terminal truncations disrupt either external Na binding to this deep site or the immediate consequences of that binding. As the occluded E1P(Na3) conformation is favored by negative voltage and elevated [Nao] (Fig. 1 B), the ∼50-mV and ∼70-mV leftward shifts of the charge curve midpoints for ΔYY and ΔKESYY truncations, respectively, reflect destabilization of the E1P(Na3) conformation relative to E2P3Na to an extent equivalent to that observed in WT (or C113Y, C113Y-ΔYY, or C113Y-ΔKESYY pumps; Fig. 10) pumps when [Nao] is lowered by a factor of approximately four or seven (Rakowski, 1993; Holmgren et al., 2000). In terms of simple access channel schemes (Gadsby et al., 1993; Rakowski, 1993; Holmgren et al., 2000; De Weer et al., 2001), the C-terminal truncations thus effectively lower the apparent affinity of the Nao binding step that limits the E2P3Na ↔ E1P(Na3) occlusion reaction by approximately four- or sevenfold. A 12–14-fold reduction in apparent affinity for Nao was recently deduced from similarly left-shifted charge–voltage curves of RD-ΔYY and RD-ΔKETYY truncated human α2 Na/K pumps (Meier et al., 2010). These shifts in equilibrium toward E2P3Na caused by the truncations could reflect acceleration of the deocclusion transition, or slowing of the occlusion transition, or both, and in energetic terms they amount to relative destabilization of E1P(Na3), in our experiments by ∼1.5–2 kT.

C-terminal truncations destabilize the occluded pump conformation containing Na ions

C-terminal truncations equivalent to ΔYY and ΔKESYY also lower the apparent affinity for cytoplasmic Na to support formation of E1P(Na3) by factors of 26 (ΔKETYY; Morth et al., 2007), 9 (ΔYY; Toustrup-Jensen et al., 2009), and ∼10 (ΔKESYY; Yaragatupalli et al., 2009), effects that suggest the truncations destabilize E1P(Na3) by ∼2–3 kT with respect to E1. The simplest explanation for these parallel relative destabilizations of the E1P(Na3) conformation with respect to both deoccluded E1 and E2P states is that the C-terminal truncations increase the free energy of the occluded Na state. In other words, the intact C terminus normally provides interactions that stabilize the E1P(Na3) state no matter how it has been formed. The results presented here, and by Meier et al. (2010), show that the two C-terminal tyrosines make the largest energetic contribution. This agrees with the suggestion of Toustrup-Jensen et al. (2009) that the reduced Na affinity of ΔYY pumps is caused predominantly by loss of cation–π stacking interactions between the aromatic rings of the two tyrosines and the guanidinium of arginine 935 (rat Na,K-ATPase numbering) in the TM8–TM9 cytoplasmic loop as well as of a hydrogen bond/salt bridge between the arginine and the C-terminal tyrosine's carboxylate. These estimates of destabilization by roughly 2 kT upon deletion of both tyrosines fall within the range of energy increases expected from loss of such interactions.

Loss of stabilizing interactions in the E1P(Na3) state caused by ΔYY and ΔKESYY truncations could also

explain the altered relaxation rates of the slow voltage jump–induced charge movements we observed in truncated pumps (Fig. 9, C and D; compare with Meier et al., 2010). The marked asymmetric voltage dependence of the exponential decay rate (the sum of forward and reverse transition rates) of the slow component of transient Na charge movement in WT Na/K pumps in high [Nao], Ko-free solutions has been ascribed to strong voltage sensitivity of the pseudo–first order transition rate of the occlusion step E2P3Na → E1P(Na3) but weak voltage sensitivity of the first order transition rate of the opposite, deocclusion step E1P(Na3) → E2P3Na. Occlusion is accelerated at increasingly negative voltages because of enhanced binding of the third Na ion deep within the electric field and thus enhanced fractional occupancy of the E2P3Na state, whereas the weak voltage dependence of the deocclusion isomerization dominates at positive potentials (Nakao and Gadsby, 1986; Rakowski, 1993; Hilgemann, 1994; Holmgren et al., 2000). In accord with this view, lowering [Nao] causes a near parallel leftward shift of the rate–voltage curve, as more negative potentials are then needed to achieve the same fractional occupancy of E2PNa3 and thus rate of occlusion, whereas the rate of deocclusion is little affected; the charge–voltage curve shows a corresponding leftward shift (Gadsby et al., 1992; Rakowski, 1993; Hilgemann, 1994; Holmgren and Rakowski, 1994; Holmgren et al., 2000). Despite temporal limitations of the two-microelectrode method for membrane voltage control in whole oocytes, the leftward shifts of the charge–voltage curves (Fig. 9, A and B) in ΔYY and ΔKESYY truncated pumps show a corresponding pattern of changes in their rate–voltage curves (Fig. 9, C and D). First, C113Y and RD pumps show small parallel leftward displacements of their rate–voltage curves compared with that of WT pumps, with slight elevation of rates at positive potentials (Fig. 9, C and D, red and green vs. black symbols); those minor changes in equilibration rates presumably underlie the similarly small shifts to the left of the charge–voltage curves of C113Y and RD pumps compared with that of WT pumps (Fig. 9, A and B). But much greater acceleration of deocclusion rates at positive potentials is seen for both ΔYY and ΔKESYY truncated pumps relative to those of their parent C113Y and RD pumps (Fig. 9, C and D). This may be expected from the aforementioned conclusion that the truncations increase the free energy of the E1P(Na3) conformation with respect to the deoccluded E2P3Na state; thus, unless the increment in energy of the transition state for deocclusion were the same as that of the occluded state, the activation free energy for deocclusion would be lowered, and the deocclusion rate therefore would be raised. By the same token, any increment in energy of the transition state for deocclusion would raise the activation free energy for occlusion, which would be expected to slow occlusion at negative potentials, as was observed, at least qualitatively, for the truncated RD pumps and to a lesser extent also for the truncated C113Y pumps (Fig. 9, C and D).

A left-shifted charge–voltage curve in ΔKESYY truncated *Xenopus* pumps, comparable with that in Fig. 9 C, was also described in another recent study (Yaragatupalli et al., 2009). However, Na/K pump current–voltage relationships in the presence and absence of Nao were not directly compared, as done in this study (Fig. 6 C), and so the attenuated influence of Nao on outward pump currents at negative potentials in ΔKESYY truncated pumps was missed. As a result, the charge–voltage curve shift was attributed to impaired Nao binding at the weakly voltage-sensitive sites shared with the two K ions, in contrast to the conclusion drawn here.

Some C-terminal mutations linked to disease similarly impair interactions with Na ions

Several mutations associated with neurological disease have recently been shown to involve the C terminus of Na/K pumps (Morth et al., 2009; compare with Tavraz et al., 2008). In a patient with sporadic hemiplegic migraine and epileptic seizures, the α2 Na,K-ATPase was found to lack the C-terminal 11 residues (Gallanti et al., 2008). A minimal C-terminal extension, the addition of a third tyrosine, was found in the α3 Na,K-ATPase of a patient with rapid-onset dystonia-parkinsonism, and even that small extension was demonstrated to impair cell survival by drastically lowering the Na/K pump's cytoplasmic Na affinity (Blanco-Arias et al., 2009). A much larger extension of the C terminus of the human α2 Na,K-ATPase by 28 residues, caused by the mutation X1021R linked to familial hemiplegic migraine type 2, was found to cause a marked leftward shift of the charge–voltage curve together with strong acceleration of charge relaxation rates at positive potentials (Tavraz et al., 2008), like the effects of the C-terminal truncations reported here and by Meier et al. (2010). X1021R may therefore also be presumed to cause destabilization of E1P(Na3). Intriguingly, mutation of the TM9 Glu (E961A; rat Na,K-ATPase numbering) proposed to contribute to the third Na ion–binding site (Ogawa and Toyoshima, 2002) resulted in similarly impaired voltage-dependent Nao binding, as assessed by comparison of Na/K pump current–voltage relationships and $K_{0.5}$(Ko)–voltage plots with and without Nao, with concomitant leftward shift of the Na charge–voltage curve and anomalous acceleration of charge relaxation at more positive voltages (Li et al., 2005). The results were interpreted as reflecting direct disruption of Na binding but are all compatible with destabilization of the occluded E1P(Na3) state as concluded here.

C-terminal truncations impair not only consequences of Nao binding but also of Ko binding

We found that the ΔYY and ΔKESYY C-terminal truncations also impaired Ko-induced closure of palytoxin-bound pump channels in the absence of ATP (Fig. 11;

compare with Artigas and Gadsby, 2003). The drop in current flow through palytoxin-bound pump channels on sudden replacement of all Nao by Ko was almost halved in magnitude in the C-terminally truncated pumps compared with RD or C113Y parent pumps (Fig. 11 and Fig. S3 B), indicating a diminished ability of Ko to lower pump channel open probability. This suggests that the gating equilibrium between open E2-like states and E2(K2)-like states, with the occlusion gate closed, is shifted away from the latter conformations back toward open-channel states. In other words, also among K-bound conformations of the pump, the C-terminal truncations cause destabilization of occluded states relative to deoccluded states.

Summary of conclusions

The unexpected location of the Na,K-ATPase's eight additional C-terminal residues compared with the SERCA Ca-ATPase suggested that their structure would make an important contribution to Na/K pump function (Morth et al., 2007). Nestled into a pocket between the cytoplasmic ends of helices TM10, TM8, and TM7, which it links to the cytoplasmic extension of TM5, the C terminus evidently provides contacts important for stabilizing Na/K pump conformations that enclose bound Na or K ions. Thus, cation-bound states are destabilized in C-terminally truncated Na/K pumps, as evident from the lowered apparent affinity with which Nai (plus ATP) or Nao generates occluded states. The reduced apparent affinity for Nao is further signaled by a diminished inhibitory influence of Nao at negative potentials on forward Na/K pumping and on Ko activation of Na/K pumping and by shifts toward more negative potentials of the voltage dependence of the slow component of pump-mediated transient charge movement in the absence of Ko. Increased free energy of occluded ion states in C-terminally truncated pumps can also account for the altered relaxation rates of that transient charge movement, which imply slowed Nao occlusion and accelerated deocclusion of Na to the exterior, as well as for the impaired ability of Ko to close the extracellular-side gate of palytoxin-bound Na/K pump channels. Under normal conditions, C-terminal truncation results in redistribution of Na/K pump conformations toward (E2P-like) states deoccluded to the exterior. This redistribution favors occasional occupancy of conformations that are apparently capable of shuttling protons across the membrane, which is evident as an inward current. A similar phenomenon can be seen even in WT Na/K pumps under appropriate conditions. Further experiments will be required to identify the conformations and mechanisms involved and to examine their relationship to proposed protonation of cation-coordinating amino acids in Na/K pumps at low cation occupancy.

We thank the late R.F. Rakowski for cDNAs encoding *Xenopus* α1 and β3 Na,K-ATPase subunits, A. Gulyás-Kovács for custom acquisition and analysis software, and N. Fataliev for molecular biological support.

This work was supported by National Institutes of Health grant HL36783 to D.C. Gadsby.

Donald H. Hilgemann served as guest editor.

Submitted: 27 January 2010
Accepted: 20 May 2010

REFERENCES

Albers, R.W. 1967. Biochemical aspects of active transport. *Annu. Rev. Biochem.* 36:727–756. doi:10.1146/annurev.bi.36.070167.003455

Apell, H.J., and A. Diller. 2002. Do H+ ions obscure electrogenic Na+ and K+ binding in the E1 state of the Na,K-ATPase? *FEBS Lett.* 532:198–202. doi:10.1016/S0014-5793(02)03675-X

Apell, H.J., and S.J. Karlish. 2001. Functional properties of Na,K-ATPase, and their structural implications, as detected with biophysical techniques. *J. Membr. Biol.* 180:1–9. doi:10.1007/s002320010053

Artigas, P., and D.C. Gadsby. 2003. Na+/K+-pump ligands modulate gating of palytoxin-induced ion channels. *Proc. Natl. Acad. Sci. USA.* 100:501–505. doi:10.1073/pnas.0135849100

Artigas, P., and D.C. Gadsby. 2004. Large diameter of palytoxin-induced Na/K pump channels and modulation of palytoxin interaction by Na/K pump ligands. *J. Gen. Physiol.* 123:357–376. doi:10.1085/jgp.200308964

Berlin, J.R., and R.D. Peluffo. 1997. Mechanism of electrogenic reaction steps during K+ transport by the NA,K-ATPase. *Ann. NY Acad. Sci.* 834:251–259. doi:10.1111/j.1749-6632.1997.tb52256.x

Blanco-Arias, P., A.P. Einholm, H. Mamsa, C. Concheiro, H. Gutiérrez-de-Terán, J. Romero, M.S. Toustrup-Jensen, A. Carracedo, J.C. Jen, B. Vilsen, and M.J. Sobrido. 2009. A C-terminal mutation of ATP1A3 underscores the crucial role of sodium affinity in the pathophysiology of rapid-onset dystonia-parkinsonism. *Hum. Mol. Genet.* 18:2370–2377. doi:10.1093/hmg/ddp170

Canessa, C.M., J.D. Horisberger, D. Louvard, and B.C. Rossier. 1992. Mutation of a cysteine in the first transmembrane segment of Na,K-ATPase alpha subunit confers ouabain resistance. *EMBO J.* 11:1681–1687.

De Weer, P., D.C. Gadsby, and R.F. Rakowski. 2001. Voltage dependence of the apparent affinity for external Na^+ of the backward-running sodium pump. *J. Gen. Physiol.* 117:315–328. doi:10.1085/jgp.117.4.315

Efthymiadis, A., J. Rettinger, and W. Schwarz. 1993. Inward-directed current generated by the Na+,K+ pump in Na(+)- and K(+)-free medium. *Cell Biol. Int.* 17:1107–1116. doi:10.1006/cbir.1993.1043

Forbush, B. III. 1984. Na+ movement in a single turnover of the Na pump. *Proc. Natl. Acad. Sci. USA.* 81:5310–5314. doi:10.1073/pnas.81.17.5310

Friedrich, T., and G. Nagel. 1997. Transient currents of Na+/K(+)-ATPase in giant patches from guinea pig cardiomyocytes induced by ATP concentration jumps or voltage pulses. *Ann. NY Acad. Sci.* 834:435–438. doi:10.1111/j.1749-6632.1997.tb52292.x

Gadsby, D.C., M. Nakao, A. Bahinski, G. Nagel, and M. Suenson. 1992. Charge movements via the cardiac Na,K-ATPase. *Acta Physiol. Scand. Suppl.* 607:111–123.

Gadsby, D.C., R.F. Rakowski, and P. De Weer. 1993. Extracellular access to the Na,K pump: pathway similar to ion channel. *Science.* 260:100–103. doi:10.1126/science.7682009

Gallanti, A., A. Tonelli, V. Cardin, G. Bussone, N. Bresolin, and M.T. Bassi. 2008. A novel de novo nonsense mutation in ATP1A2 associated with sporadic hemiplegic migraine and epileptic seizures. *J. Neurol. Sci.* 273:123–126. doi:10.1016/j.jns.2008.06.006

Garrahan, P.J., and I.M. Glynn. 1967. Factors affecting the relative magnitudes of the sodium:potassium and sodium:sodium exchanges catalysed by the sodium pump. *J. Physiol.* 192:189–216.

Glynn, I.M. 1993. Annual review prize lecture. 'All hands to the sodium pump'. *J. Physiol.* 462:1–30.

Heyse, S., I. Wuddel, H.J. Apell, and W. Stürmer. 1994. Partial reactions of the Na,K-ATPase: determination of rate constants. *J. Gen. Physiol.* 104:197–240. doi:10.1085/jgp.104.2.197

Hilgemann, D.W. 1994. Channel-like function of the Na,K pump probed at microsecond resolution in giant membrane patches. *Science.* 263:1429–1432. doi:10.1126/science.8128223

Holmgren, M., and R.F. Rakowski. 1994. Pre-steady-state transient currents mediated by the Na/K pump in internally perfused *Xenopus* oocytes. *Biophys. J.* 66:912–922. doi:10.1016/S0006-3495(94)80867-7

Holmgren, M., and R.F. Rakowski. 2006. Charge translocation by the Na+/K+ pump under Na+/Na+ exchange conditions: intracellular Na+ dependence. *Biophys. J.* 90:1607–1616. doi:10.1529/biophysj.105.072942

Holmgren, M., J. Wagg, F. Bezanilla, R.F. Rakowski, P. De Weer, and D.C. Gadsby. 2000. Three distinct and sequential steps in the release of sodium ions by the Na+/K+-ATPase. *Nature.* 403:898–901. doi:10.1038/35002599

Imagawa, T., T. Yamamoto, S. Kaya, K. Sakaguchi, and K. Taniguchi. 2005. Thr-774 (transmembrane segment M5), Val-920 (M8), and Glu-954 (M9) are involved in Na+ transport, and Gln-923 (M8) is essential for Na,K-ATPase activity. *J. Biol. Chem.* 280:18736–18744. doi:10.1074/jbc.M500137200

Jaisser, F., P. Jaunin, K. Geering, B.C. Rossier, and J.D. Horisberger. 1994. Modulation of the Na,K-pump function by β subunit isoforms. *J. Gen. Physiol.* 103:605–623. doi:10.1085/jgp.103.4.605

Jorgensen, P.L., and P.A. Pedersen. 2001. Structure-function relationships of Na(+), K(+), ATP, or Mg(2+) binding and energy transduction in Na,K-ATPase. *Biochim. Biophys. Acta.* 1505:57–74. doi:10.1016/S0005-2728(00)00277-2

Kaplan, J.H. 2002. Biochemistry of Na,K-ATPase. *Annu. Rev. Biochem.* 71:511–535. doi:10.1146/annurev.biochem.71.102201.141218

Li, C., O. Capendeguy, K. Geering, and J.D. Horisberger. 2005. A third Na+-binding site in the sodium pump. *Proc. Natl. Acad. Sci. USA.* 102:12706–12711. doi:10.1073/pnas.0505980102

Li, C., K. Geering, and J.D. Horisberger. 2006. The third sodium binding site of Na,K-ATPase is functionally linked to acidic pH-activated inward current. *J. Membr. Biol.* 213:1–9. doi:10.1007/s00232-006-0035-0

Meier, S., N.N. Tavraz, K.L. Dürr, and T. Friedrich. 2010. Hyperpolarization-activated inward leakage currents caused by deletion or mutation of carboxy-terminal tyrosines of the Na^+/K^+-ATPase α subunit. *J. Gen. Physiol.* 135:115–134. doi:10.1085/jgp.200910301

Morth, J.P., B.P. Pedersen, M.S. Toustrup-Jensen, T.L. Sørensen, J. Petersen, J.P. Andersen, B. Vilsen, and P. Nissen. 2007. Crystal structure of the sodium-potassium pump. *Nature.* 450:1043–1049. doi:10.1038/nature06419

Morth, J.P., H. Poulsen, M.S. Toustrup-Jensen, V.R. Schack, J. Egebjerg, J.P. Andersen, B. Vilsen, and P. Nissen. 2009. The structure of the Na+,K+-ATPase and mapping of isoform differences and disease-related mutations. *Philos. Trans. R. Soc. Lond. B Biol. Sci.* 364:217–227. doi:10.1098/rstb.2008.0201

Nakao, M., and D.C. Gadsby. 1986. Voltage dependence of Na translocation by the Na/K pump. *Nature.* 323:628–630. doi:10.1038/323628a0

Nakao, M., and D.C. Gadsby. 1989. [Na] and [K] dependence of the Na/K pump current-voltage relationship in guinea pig ventricular myocytes. *J. Gen. Physiol.* 94:539–565. doi:10.1085/jgp.94.3.539

Ogawa, H., and C. Toyoshima. 2002. Homology modeling of the cation binding sites of Na+K+-ATPase. *Proc. Natl. Acad. Sci. USA.* 99:15977–15982. doi:10.1073/pnas.202622299

Ogawa, H., T. Shinoda, F. Cornelius, and C. Toyoshima. 2009. Crystal structure of the sodium-potassium pump (Na+,K+-ATPase) with bound potassium and ouabain. *Proc. Natl. Acad. Sci. USA.* 106:13742–13747. doi:10.1073/pnas.0907054106

Olesen, C., T.L. Sørensen, R.C. Nielsen, J.V. Møller, and P. Nissen. 2004. Dephosphorylation of the calcium pump coupled to counterion occlusion. *Science.* 306:2251–2255. doi:10.1126/science.1106289

Olesen, C., M. Picard, A.M. Winther, C. Gyrup, J.P. Morth, C. Oxvig, J.V. Møller, and P. Nissen. 2007. The structural basis of calcium transport by the calcium pump. *Nature.* 450:1036–1042. doi:10.1038/nature06418

Peluffo, R.D., and J.R. Berlin. 1997. Electrogenic K+ transport by the Na(+)-K+ pump in rat cardiac ventricular myocytes. *J. Physiol.* 501:33–40. doi:10.1111/j.1469-7793.1997.033bo.x

Post, R.L., A.K. Sen, and A.S. Rosenthal. 1965. A phosphorylated intermediate in adenosine triphosphate-dependent sodium and potassium transport across kidney membranes. *J. Biol. Chem.* 240:1437–1445.

Post, R.L., C. Hegyvary, and S. Kume. 1972. Activation by adenosine triphosphate in the phosphorylation kinetics of sodium and potassium ion transport adenosine triphosphatase. *J. Biol. Chem.* 247:6530–6540.

Price, E.M., and J.B. Lingrel. 1988. Structure-function relationships in the Na,K-ATPase alpha subunit: site-directed mutagenesis of glutamine-111 to arginine and asparagine-122 to aspartic acid generates a ouabain-resistant enzyme. *Biochemistry.* 27:8400–8408. doi:10.1021/bi00422a016

Rakowski, R.F. 1993. Charge movement by the Na/K pump in *Xenopus* oocytes. *J. Gen. Physiol.* 101:117–144. doi:10.1085/jgp.101.1.117

Rakowski, R.F., and S. Sagar. 2003. Found: Na(+) and K(+) binding sites of the sodium pump. *News Physiol. Sci.* 18:164–168.

Rakowski, R.F., D.C. Gadsby, and P. De Weer. 1989. Stoichiometry and voltage dependence of the sodium pump in voltage-clamped, internally dialyzed squid giant axon. *J. Gen. Physiol.* 93:903–941. doi:10.1085/jgp.93.5.903

Rakowski, R.F., L.A. Vasilets, J. LaTona, and W. Schwarz. 1991. A negative slope in the current-voltage relationship of the Na+/K+ pump in *Xenopus* oocytes produced by reduction of external [K+]. *J. Membr. Biol.* 121:177–187. doi:10.1007/BF01870531

Rettinger, J. 1996. Characteristics of Na+/K(+)-ATPase mediated proton current in Na(+)- and K(+)-free extracellular solutions. Indications for kinetic similarities between H+/K(+)-ATPase and Na+/K(+)-ATPase. *Biochim. Biophys. Acta.* 1282:207–215. doi:10.1016/0005-2736(96)00057-0

Sagar, A., and R.F. Rakowski. 1994. Access channel model for the voltage dependence of the forward-running Na^+/K^+ pump. *J. Gen. Physiol.* 103:869–893. doi:10.1085/jgp.103.5.869

Shinoda, T., H. Ogawa, F. Cornelius, and C. Toyoshima. 2009. Crystal structure of the sodium-potassium pump at 2.4 A resolution. *Nature.* 459:446–450. doi:10.1038/nature07939

Sørensen, T.L., J.V. Møller, and P. Nissen. 2004. Phosphoryl transfer and calcium ion occlusion in the calcium pump. *Science.* 304:1672–1675. doi:10.1126/science.1099366

Starace, D.M., and F. Bezanilla. 2004. A proton pore in a potassium channel voltage sensor reveals a focused electric field. *Nature.* 427:548–553. doi:10.1038/nature02270

Steinberg, M., and S.J. Karlish. 1989. Studies on conformational changes in Na,K-ATPase labeled with 5-iodoacetamidofluorescein. *J. Biol. Chem.* 264:2726–2734.

Stürmer, W., R. Bühler, H.J. Apell, and P. Läuger. 1991. Charge translocation by the Na,K-pump: II. Ion binding and release at the extracellular face. *J. Membr. Biol.* 121:163–176. doi:10.1007/BF01870530

Takeuchi, A., N. Reyes, P. Artigas, and D.C. Gadsby. 2008. The ion pathway through the opened Na(+),K(+)-ATPase pump. *Nature.* 456:413–416. doi:10.1038/nature07350

Taniguchi, K., and R.L. Post. 1975. Synthesis of adenosine triphosphate and exchange between inorganic phosphate and adenosine

triphosphate in sodium and potassium ion transport adenosine triphosphatase. *J. Biol. Chem.* 250:3010–3018.

Tavraz, N.N., T. Friedrich, K.L. Dürr, J.B. Koenderink, E. Bamberg, T. Freilinger, and M. Dichgans. 2008. Diverse functional consequences of mutations in the Na+/K+-ATPase alpha2-subunit causing familial hemiplegic migraine type 2. *J. Biol. Chem.* 283: 31097–31106. doi:10.1074/jbc.M802771200

Toustrup-Jensen, M.S., R. Holm, A.P. Einholm, V.R. Schack, J.P. Morth, P. Nissen, J.P. Andersen, and B. Vilsen. 2009. The C terminus of Na+,K+-ATPase controls Na+ affinity on both sides of the membrane through Arg935. *J. Biol. Chem.* 284:18715–18725. doi:10.1074/jbc.M109.015099

Toyoshima, C., and T. Mizutani. 2004. Crystal structure of the calcium pump with a bound ATP analogue. *Nature.* 430:529–535. doi:10.1038/nature02680

Toyoshima, C., and H. Nomura. 2002. Structural changes in the calcium pump accompanying the dissociation of calcium. *Nature.* 418:605–611. doi:10.1038/nature00944

Toyoshima, C., M. Nakasako, H. Nomura, and H. Ogawa. 2000. Crystal structure of the calcium pump of sarcoplasmic reticulum at 2.6 A resolution. *Nature.* 405:647–655. doi:10.1038/35015017

Toyoshima, C., H. Nomura, and T. Tsuda. 2004. Lumenal gating mechanism revealed in calcium pump crystal structures with phosphate analogues. *Nature.* 432:361–368. doi:10.1038/nature02981

Toyoshima, C., Y. Norimatsu, S. Iwasawa, T. Tsuda, and H. Ogawa. 2007. How processing of aspartylphosphate is coupled to lumenal gating of the ion pathway in the calcium pump. *Proc. Natl. Acad. Sci. USA.* 104:19831–19836. doi:10.1073/pnas.0709978104

Vasilyev, A., K. Khater, and R.F. Rakowski. 2004. Effect of extracellular pH on presteady-state and steady-state current mediated by the Na+/K+ pump. *J. Membr. Biol.* 198:65–76. doi:10.1007/s00232-004-0660-4

Vilsen, B. 1992. Functional consequences of alterations to Pro328 and Leu332 located in the 4th transmembrane segment of the alpha-subunit of the rat kidney Na+,K(+)-ATPase. *FEBS Lett.* 314:301–307. doi:10.1016/0014-5793(92)81494-7

Wang, X., and J.D. Horisberger. 1995. A conformation of Na(+)-K+ pump is permeable to proton. *Am. J. Physiol.* 268:C590–C595.

Wuddel, I., and H.J. Apell. 1995. Electrogenicity of the sodium transport pathway in the Na,K-ATPase probed by charge-pulse experiments. *Biophys. J.* 69:909–921. doi:10.1016/S0006-3495(95)79965-9

Yaragatupalli, S., J.F. Olivera, C. Gatto, and P. Artigas. 2009. Altered Na+ transport after an intracellular alpha-subunit deletion reveals strict external sequential release of Na+ from the Na/K pump. *Proc. Natl. Acad. Sci. USA.* 106:15507–15512. doi:10.1073/pnas.0903752106